EXPERIMENTAL FREQUENCY RESPONSE OF FLUID LINES

BY

Qizhao Li

A Thesis
Submitted to the Faculty of Graduate Studies
In Partial Fulfillment of the Requirements for the Degree of

Master of Science
In
Mechanical Engineering

Department of Mechanical and Manufacturing Engineering
University of Manitoba
Winnipeg, Manitoba
Canada

THE UNIVERSITY OF MANITOBA

FACULTY OF GRADUATE STUDIES

****

COPYRIGHT PERMISSION PAGE

Experimental Frequency Response of Fluid Lines

By

Qizhao Li

A Thesis/Practicum submitted to the Faculty of Graduate Studies of The University of Manitoba in partial fulfillment of the requirements of the degree

of

Master of Science

ABSTRACT

The study of transient pipe flow is of practical significance because of their many important applications, such as surging phenomena or waterhammer in power plants, aerodynamics, liquid-propellant rocket systems, and hydraulic and pneumatic control systems, etc. In this thesis, a test facility has been constructed to measure the frequency response of laminar and turbulent transient pipe flows. Frequency responses of three test lines were measured in the frequency range of 2-500 Hz. The experiment using a dead-end line is compared with a simple transfer function solution, and it reveals the effects of frequency-dependent damping. Results of an experiment in turbulent flow and a corresponding laminar experiment are presented for further research.

ACKNOWLEDGEMENTS

I would like to express my sincere acknowledgments and gratitude to my advisor Dr. Chatoorgoon V for giving me the opportunity to work in this challenging field of research. His invaluable help in all aspects, for being patient and strenuous to get the best out of me.

I would like to thank my parents and sisters who gave me a lot of moral support making me come out with flying colors.

I would like to thank all my friends all through my life who have been really supportive and given me a helping hand at hard times.

DEDICATION

I whole heartedly dedicate my thesis to my beloved parents Xiaofei Li and Jingyan Li.

TABLE OF CONTENTS

LIST OF FIGURES

LIST OF TABLES

NOMENCLATURE

P_0	Amplitude of the upstream dynamic pressure (Pa)
P_1	Amplitude of the downstream dynamic pressure (Pa)
P_1/P_0	Dynamic pressure amplification
L	Length of the test line (m)
P	System pressure (MPa)
T	Water temperature (°C)
Re	Reynolds number
$\Gamma(s)$	The propagation operator
Z(s)	The characteristic impedance
Ψ	The nondimensional parameter which defines the elastic properties of the line
R_P	The resistance per unit length of the line
K	Water Bulk Modulus of Elasticity (GPa)
E	Line Young's Modulus of Elasticity (GPa)
R	The outside radius of the pipe (m)
r	The inside radius of the pipe (m)
c	The speed of sound in the line (m/s)
u′	Dynamic velocity (m/s)
P′	Dynamic pressure (MPa)
ρ	Water Density (Kg/m^3)
υ	Water Viscosity ($Pa.S\times10^{-6}$)
ν	Line Poisson's Ratio

ζ	Resistance Coefficient for Line Elements
z	The function variable
j	The complex number
s	The complex, Fourier variable
w	The angular frequency (Radian/Second)
f_R	The resonant frequency (Hz)
f_M	The minimum amplification frequency (Hz)
Δf	The resonant frequency shift (Hz)

CHAPTER ONE: Introduction

The study of transient pipe flow is of practical significance because of their many important applications, such as surging phenomena or waterhammer in piping systems, aerodynamics, liquid-propellant rocket systems, and hydraulic and pneumatic control systems, etc. In transient flow caused by accidental or normal pump trips, pump start and rapid changes in valve settings, the flow velocity and pressure in a pipe system changes rapidly. Fast moving pressure waves are generated and move through the system at speeds up to the speed of sound. In practice, many factors can generate unsteady pressures on internal surface of a pipe, such as turbulence, cavitation, vortex shedding, valve chatter, and the passing of pump impeller vanes.

Depending on the piping geometry, acoustic resonant conditions may occur, potentially producing large pressure pulsations that excite the piping system. If the exciting frequency coincides with the natural frequency of the system, resonance will occur creating, possibly, large forces on the piping. Large pressure oscillations may cause rapture or collapse of the pipes. A notable example of such an acoustic resonance was observed in the Primary Heat Transport (PHT) system at Ontario Power Generation Darlington nuclear power station [1, 2, 3]. The fatigue failures in the fuel bundle end plates, and ultimately the breakup, of some nuclear fuel bundles were identified to be caused by acoustic excitation in the piping system.

The study of transient flow has been of continuous interest since the early part of the nineteenth century. Depending on the interest, two different but related analyses, frequency response analysis and free vibration analysis, were performed. The frequency response analysis is based on fully developed steady oscillatory forced vibrations. It involves simulating a variation of a pressure head and flow in a fluid system due to an explicit forced excitation. Free vibration analyses investigate a free-oscillatory fluid motion. Free vibration analysis does not inquire into the nature of the forcing function, but determines natural frequencies of a system and provides information on a stability of the systems and on a rate of attenuation or amplification of the oscillations.

By borrowing procedures from linear vibration theory and electrical transmission-line theory, the classic theory for transient flow based on the Navier-Stokes equations was well developed in a time domain and frequency domain. Thus, several analytical approaches have been proposed for frequency response and free vibration analyses, such as the transfer function method, the method of characteristics, the finite element/difference solution of the governing equations, etc. Nevertheless, experimental validation of theoretic analyses has shown significant discrepancies in attenuation and phase shift of pressure traces. The primary reason for this lack of agreement is believed to be frictional effects. The magnitude of discrepancies is governed by flow conditions (fast or slow transients, laminar or turbulent flow, and oscillating frequencies) and liquid properties (viscosity).

Researchers developed a number of unsteady friction models to simulate the behavior of transient flow by relating damping effects with different flow conditions (fast or slow transients, laminar or turbulent flow) and liquid properties (viscosity). The unsteady damping models can be classified into six groups:

(1) The friction term is dependent on the instantaneous mean flow velocity and the instantaneous local acceleration [4, 5].

(2) The friction term is dependent on the instantaneous mean flow velocity [6, 7, 8, 9, 10, 11, 12, 13].

(3) The friction term is based on the cross-sectional distribution of instantaneous flow velocity [14, 15, 16, 17, 18, 19, 20, 21, 22, 23, 24, 25, 26, 27, 28, 29, 30, 31].

(4) The friction term is dependent on the instantaneous mean flow velocity and weights for past velocity changes [32, 33, 34, 35, 36, 37, 38, 39, 40, 41, 42].

(5) The friction term is dependent on the instantaneous mean flow velocity, the instantaneous local acceleration and the instantaneous convective acceleration [43, 44, 45].

(6) The friction term is dependent on the instantaneous mean flow velocity and the diffusion [46, 47].

Because of the complicated velocity distribution in the boundary layers, these models are deficient in describing the friction effect in transient flows, especially for high Reynolds number turbulent flow and oscillating frequencies in the 100-500 Hz range. Experiments under high Reynolds number turbulent flow and high oscillating

frequencies are needed to help develop damping models in transient flow.

To study an acoustic wave in both laminar and turbulent flows, three experiments are performed in single straight test lines in laminar and turbulent flows, in the frequency range of 2-500 Hz. The experiment using dead-end test line is compared with a simple transfer function solution. The results are discussed. Results of experiments in turbulent flow and a corresponding laminar experiment are presented for further research. Some interesting phenomena are discussed for further theoretical simulation.

1.1 Objective

The objective of this work is:

To do 'simple' and 'clean' experiments, with low levels of uncertainty and minimal miscellaneous effects, of acoustic wave damping in laminar and turbulent pipe flows for developing more accurate damping models of acoustic wave propagation.

1.2 Reviews

1.2.1 Literature Review

The study of wave propagation in lines has been of interest since the early part of the nineteenth century. In 1808, Young [48] estimated the speed of propagation of an impulse in an elastic line. After the development of the basic equations of fluid

mechanics by Navier and Stokes around 1850, significant advances were possible considering the fluid as compressible [52]. By the early part of the twentieth century, the theory of waterhammer was well developed. Hence, by borrowing the procedures from classic wave theory and the theory of transmission lines, the basic theory for transient flow was well in hand.

The frequency response analysis is based on fully developed steady-oscillatory forced vibrations. The forcing exciter, which is known a priori, may be an induced flow or pressure oscillation, or a forced relationship between the two variables as may be imposed by an oscillating valve. The excited dynamic pressures and flow velocities vary harmonically at each point in the system at the frequency of the excitation, and they are independent of time while the steady oscillation is maintained by the forcing function, neither decaying nor amplifying in time. Hence, the objective of the frequency response analysis is to compute the variation of the dynamic pressures and flow velocities in a fluid system due to an explicit excitation imposed on the system.

The governing equations used to describe the behavior of oscillating flows are: momentum, continuity, state and, if heat transfer is considered, energy equations. Based on these fundamental equations, several analytical approaches have been proposed, such as the transfer function method, the method of characteristics, the finite element/difference solution of the governing equations, etc. The study of damping effects in transient flow became the main difficulty in the theory development.

In the past decades, a number of damping models for transient flow have been developed. These models affect acoustic damping through the friction terms in the Navier-Stokes equations. A brief review of these damping models is presented next.

1.2.1.1 Damping Models for Laminar Flow

For frequency response analysis, D'Souza and Oldenburger [9] used the linearized Navier-Stokes equations, transformed in the LaPlacian domain, and derived frequency response equations for laminar flow, which included the effects of fluid viscosity. By comparisons with experiments, they showed increased damping effects due to fluid viscosity and frequency and showed that correct amplitudes can be achieved by paying proper attention to the viscous shear-stress terms. Foster and Parker [10] derived a formula to calculate the volumetric drag coefficient for laminar flow. The work of Philips and Chiang [12] was in a similar vein, except that they derived analytic expressions for the instantaneous, time dependent friction factor as a function of frequency.

Zielke [32] made an important contribution to modeling friction effects of waterhammer waves. He derived a frequency-dependent friction model for transient laminar flow in which the friction term is related to the instantaneous mean flow velocity and weights of past velocity changes. The advantages of this approach are that there is no need for empirical coefficients and the friction term is suitable for the

frequency domain. The Zielke model in both the frequency and time domains had a great influence on later studies.

However, Zielke's model requires excessive computer storage and computation time in the simulation with the method of characteristics, and may be considered time-consuming for the analysis of large systems. Various researchers modified the Zielke model to improve computational efficiency for transient laminar flow. Trikha [33] improved Zielke's model by an efficient procedure for simulating frequency-dependent friction. The procedure consists of approximating Zielke's weighting function by a series of simple exponential expressions for frequency-dependent friction to save calculation cost. Kagawa [34] improved Zielke's method by approximating Zielke's weighting functions by a sum of impulse responses of first order lag system. Suzuki et al. [36] simplified the Zielke weighting function by a mathematically equivalent calculation without approximation. It saved calculation cost and kept the accuracy. Schohl [39] derived a five-term approximation to the weighting function in the original Zielke's model. By introducing the formulae of wall shear stress for unsteady laminar pipe flow from other researchers, Shuy [40] developed a simple approximation to the weighting function in Zielke's model in terms of the instantaneous section mean velocity and acceleration.

Various authors used two-dimensional approaches to study the unsteady friction based on particular representations of wall layer in laminar flow. Ohmi [16] introduced four characteristic parameters to describe the flow patterns in a pulsating

pipe flow, and this flow patterns were classified into three types, i.e., quasi-steady, intermediate, and inertia dominant ones with respect to a dimensionless frequency. Based on the flow patterns, Ohmi [20, 21] derived a multilayer model with different analytical representations for wall shear stress and friction loss. Bratland [26] developed a multilayer friction model to account for the frequency-dependence of the friction and the radial variation of the kinetic energy for simulating transient compressible pipe flow. Eichinger and Lein [27] developed a friction model by using empirical k-ε models to calculate the cross-sectional distribution of instantaneous flow velocity, for laminar and low Reynolds number turbulent pipe flows. Silver-Araya and Chaudhry [30] developed a numerical model by using two-region empirical k-ε models to estimate the instantaneous velocity profiles and the energy dissipation for laminar and turbulent flows.

1.2.1.2 Damping Models for Turbulent Flow

A great effort has been contributed to the transient response of turbulent pipe flow with frequency-dependent friction since early 1930s. Several linear steady friction models were developed for simulating frictional effects in turbulent flow by Wood [7], Rich [8], etc. In these models, the friction term is proportional to the velocity transients. Wood [7] concluded that the approximation of the viscous effects by the linear term provided a mechanism for including dissipation but was deficient in accurately predicting the exact viscous effects.

An early unsteady friction model was developed by Daily et al. [4] for turbulent flow, in which experimental resistance coefficients dependent on instantaneous mean flow velocity and instantaneous local acceleration were used. Brown et al. [11, 13] used semi-empirical analytical models to investigate viscous effects for small-amplitude sinusoidal disturbances in turbulent flow. By comparison with experiments, researchers realized that the behavior of unsteady friction is more complicated in turbulent flow than in laminar flow because of the complicated velocity distribution in the boundary at high Reynolds number turbulent flow and high oscillating frequency.

Influenced by Zielke's model, various researchers improved the weighting function for turbulent flow. Brown [35] extended Zielke's weighting function to turbulent flow with experimental frequency-dependent friction factors. With several five-region approximations, Vardy et al. [37, 38, 41, 42] developed several weighting function models of transient friction for different Reynolds number range. Brunone [43] developed a viscous loss model by assuming a quasi-steady contribution and an unsteady contribution that is related to the instantaneous acceleration and the instantaneous convective acceleration. Wylie [49] developed a clear implementation procedure for the model proposed by Brunone.

With the development of measurement techniques and the advent of fast and inexpensive computer, a number of two-dimensional models were developed by researchers. Different from one-dimensional models, in which empirical coefficients

or weighting functions are used to describe the instantaneous cross-sectional velocity profile, the 2D models separate pipe flow into several layers and use analytic and experimental approximations to compute the actual velocity profile and corresponding energy losses during the transient process.

Wood and Funk [14] developed a two-region model for general transient turbulent flow conditions in a tube. A simple laminar boundary-layer model was used to describe the viscous effects. It was found that the model was deficient in high Reynolds number turbulent flows, and revealed that turbulent boundary layers can not be simplified as laminar boundary layers.

Ohmi et al. [15] developed an eddy viscosity model by using the instantaneous velocity profile to calculate the steady and oscillating eddy viscosity for low frequency pulsating turbulent pipe flow. The velocity profile was simulated by a four-region approximation and finite difference method was used. Furthermore, to investigate the effect of pulsating frequency, four characteristic parameters were introduced to describe the flow pattern in a pulsating turbulent pipe flow, and the flow patterns were classified into three types, i.e., quasi-steady, intermediate, and inertia dominant ones with respect to a dimensionless frequency [16]. Frequency-dependent friction models were developed based on the flow patterns in the turbulent pipe flow [17, 18, 19, 22, 23, 25].

Vardy and Hwang [28] developed a quasi two-dimensional friction model for laminar and low Reynolds number turbulent flow. Lateral velocity components are calculated between adjacent cylinders and the relationship between shear stress and local velocities is applied to laminar flows and to a five-region model of turbulent flow.

Zhou [29] developed a two-region damping model to predict the volumetric drag in turbulent 'rough' pipe flow. Pezzinga [31] developed a quasi two-dimensional model basing on the mixing length hypothesis in turbulent zone and on Newton's law in the viscous sublayer. Chen and Veshagh [50] developed a two-region friction model by using the law of the wake to describe the instantaneous velocity profile of the core region and the law of the wall for the wall region.

Hino et al. [6] developed a friction model in which the friction term is dependent on the instantaneous mean flow velocity. Bughazen and Anderson [44] developed several friction models by relating the friction term with instantaneous mean flow velocity, instantaneous local acceleration and instantaneous convective acceleration. In the work of Vennatro [46] and Svingen [47], the friction term was related to the instantaneous mean flow velocity and diffusion. Suo and Wylie [51] developed an impulse response method in which frequency-dependent parameters influence the response. Goodson et al. [52] and Bergant et al. [53, 54] provided detailed reviews of the development of the friction models.

However, the application of most friction models described above was focused on

waterhammer analysis. The experiments validations of these models were also performed under conditions of very low frequency (i.e., less than 50Hz) which are suitable for waterhammer phenomena. The friction model for frequency response analysis under high oscillating frequency and high Reynolds number turbulent flow is unfolding. Chatoorgoon [55, 56, 57] utilized several damping models in TARA and ABAQUS to simulate the behavior of oscillating turbulent flow for practical problems and pointed out that experiments for validating these models are urgently required.

1.2.2 Previous Experiments

Over past fifty years, various experiments were performed to study the behavior of acoustic wave propagation in fluid line. By measuring the pressure loss and velocity profile, the damping effects in unsteady pipe flows were studied experimentally [4, 11, 13, 14, 16, 58, 59, 60, 61, 62, 63, 64, 65, 66, 67] at different flow condition (laminar or turbulent) and oscillating frequencies. For waterhammer application, various experiments at different initial values of flow (laminar or turbulent), different piping systems, different valve actions (opening or closing) and different closure times were performed [5, 45, 68, 69, 70, 71, 72, 73, 74, 75, 76, 77]. For acoustic waves produced by pumps, several experiments were carried out [78, 79, 80, 81, 82].

As previously mentioned, the above experiments were mostly performed at low oscillating frequencies. In practice, unsteady transient flow can occur in a broad frequency range, such as the acoustic resonance problems in the Darlington nuclear

power station in which the resonance frequencies were found ranging from 100 to 300Hz.

To the author's knowledge, five frequency response experiments were reported: experiments of Ontario Hydro Research Division (OHRD) [2], D'Souza and Oldenburger [9], Washio and Konishi [83], Rzentkowski [84], and Stern Lab [85, 86]. The experimental setup and conditions of the experiments are briefly listed in Table 1.

D'Souza and Oldenburger [9], Washio and Konishi [83], Rzentkowski [84] measured the frequency responses of a single straight test line at different flow condition and boundary condition.

To solve the accidents caused by acoustic excitation in PHT system at Darlington nuclear power station, full-scale tests of PHT piping system were performed at OHRD [2]. Dynamic pressure pulses, piping vibration, pump/motor vibration and mean flow velocities were measured under different operating conditions.

Stern Lab set up a mock-up of the Darlington 'K12' fuel feed channel to simulate the 'real life' complicated situation in CANDU station [85, 86]. The experimental setup consisted of a single fuel channel with inlet and outlet feeders, flanges, reducers, bends and branches, etc. Dynamic pressure pulses, piping vibration and mean flow velocities were measured under different operating conditions.

Table 1: Experiment Setup and Conditions of Previous Experiments

Experiment		D'Souza et al. [9]	Washio et al. [83]	Rzentkowski [84]	OHRD [2]	Stern Lab [85, 86]
Setup	Material	Stainless-Steel	Steel	Type 304 Stainless Steel	Full-scale tests of Darlington PHT system design solutions	A mock-up of the Darlington 'K12' Channel
	Length	40.25 ft	3.18 m	7.08 m and 12.80 m		
	Diameter	0.495 in I.D., 0.065 in Wall Thickness	21.6 mm I.D., 2.8 mm wall thickness	9.52 mm O.D., 7.04 mm I.D.		
	Direction	Horizontally	Vertically	Horizontally		
	Boundary Conditions	A fabricated orifice located at the downstream end	Dead-end at downstream end; With steel rods (15 & 8 mm diameter) coaxially fixed in pipe.	Dead-end at downstream end		
Flow	Fluid	Hydraulic oil Mil-0-5606	Turbine oil No. 2	Water	Demineralized water	Regular GE fuel
	System Pressure	225 Psig	—	400 kPa	9.56 MPa	—
	Temperature	83 °F	20 °C	22 °C	25-280 °C	60-290 °C
	Flow Type	Laminar	0	0	Turbulent	Turbulent
Frequency Range (Hz)		0-100	0-600	0-500	0-250	100-240

1.2.3 Conclusions

The information deduced from previous review can therefore be summarized as follows:

(1) In transient flow, the friction effect becomes unsteady. It is a function of flow conditions, liquid properties, and frequency dependent.

(2) Acoustic damping in laminar flow is better understood than acoustic damping in turbulent flow. The effect of frictional contribution in turbulent flow damping need to be further researched.

(3) For improving damping models in turbulent flow and broad frequency range, "simple" and "clean" experiment with low levels of uncertainty are urgently needed.

(4) The effect of geometric changes, bends and branches in piping system on friction effects and reflected acoustic waves are not fully understood and needed to be studied.

CHAPTER TWO: Experiment

2.1 Experimental Set-Up

To investigate the characteristics of frequency response in both laminar and turbulent pipe flows, a test facility was constructed and is shown schematically in Figures 1 and 2.

2.1.1 Shaker and Cylinder

A cylinder, driven by a LDS V408 Model electromechanical shaker, was located at the upstream end of the test lines to produce the oscillating pressure waves. The shaker was fixed by a specially designed steel support to minimize its vibration. The cylinder was pressurized on its both sides, by connecting to the water-feed loop, to balance the applied force on the shaker.

2.1.2 Test Lines

Test lines used were made of 304L stainless steel pipes with an inner diameter of 7.23 mm and an outside diameter of 8.50 mm. Two test lines were used: 7.03 m in length (the same length with the test line used in Rzentkowski's experiment [84]) and 9.20 m in length. The test lines were supported at 25 cm intervals by cushioned clamps to minimize line vibration. A short rubber hose (~3.5cm long) was located between the cylinder

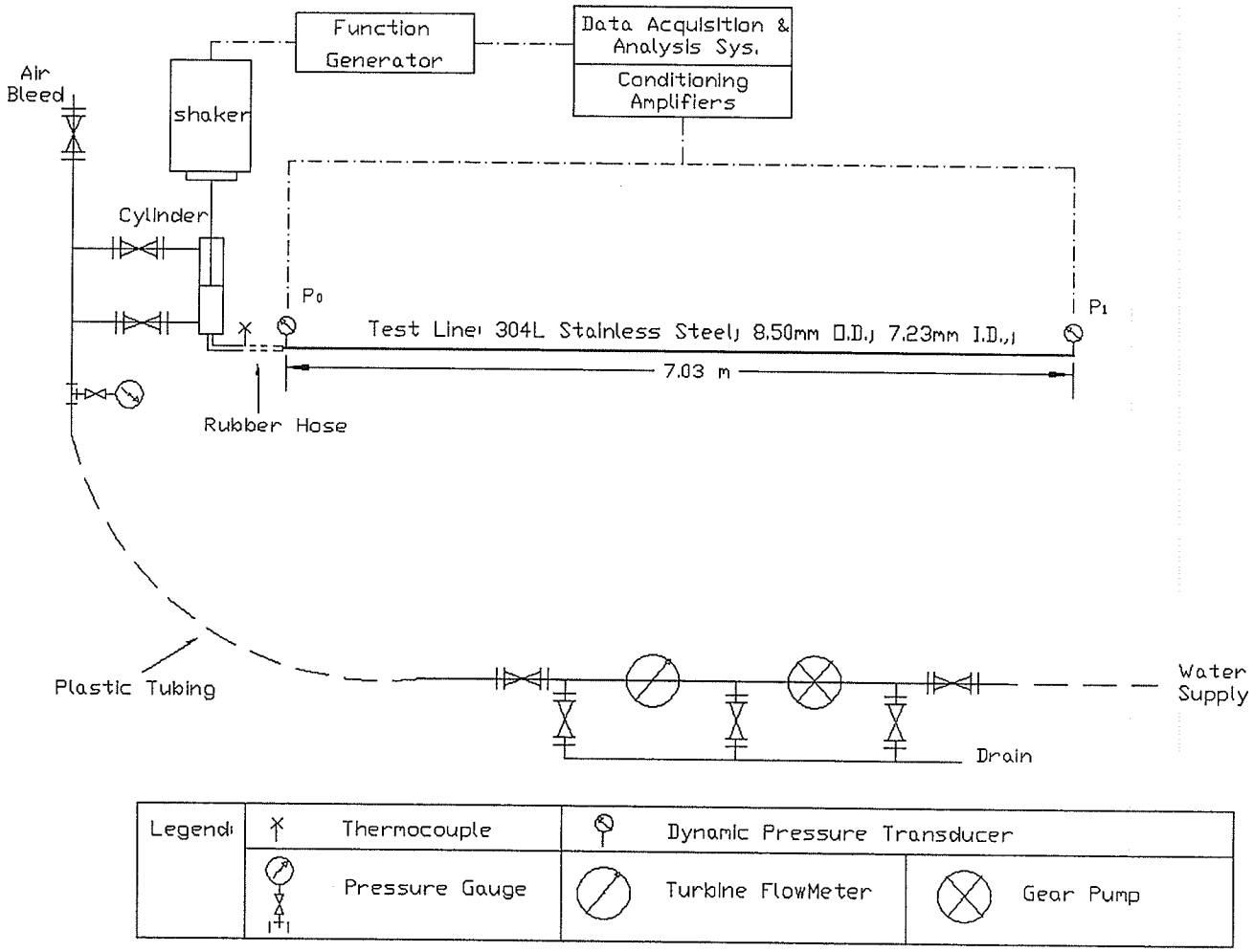

Figure 1: Schematic Diagram of The '7.03 m Dead-End Experiment' Setup

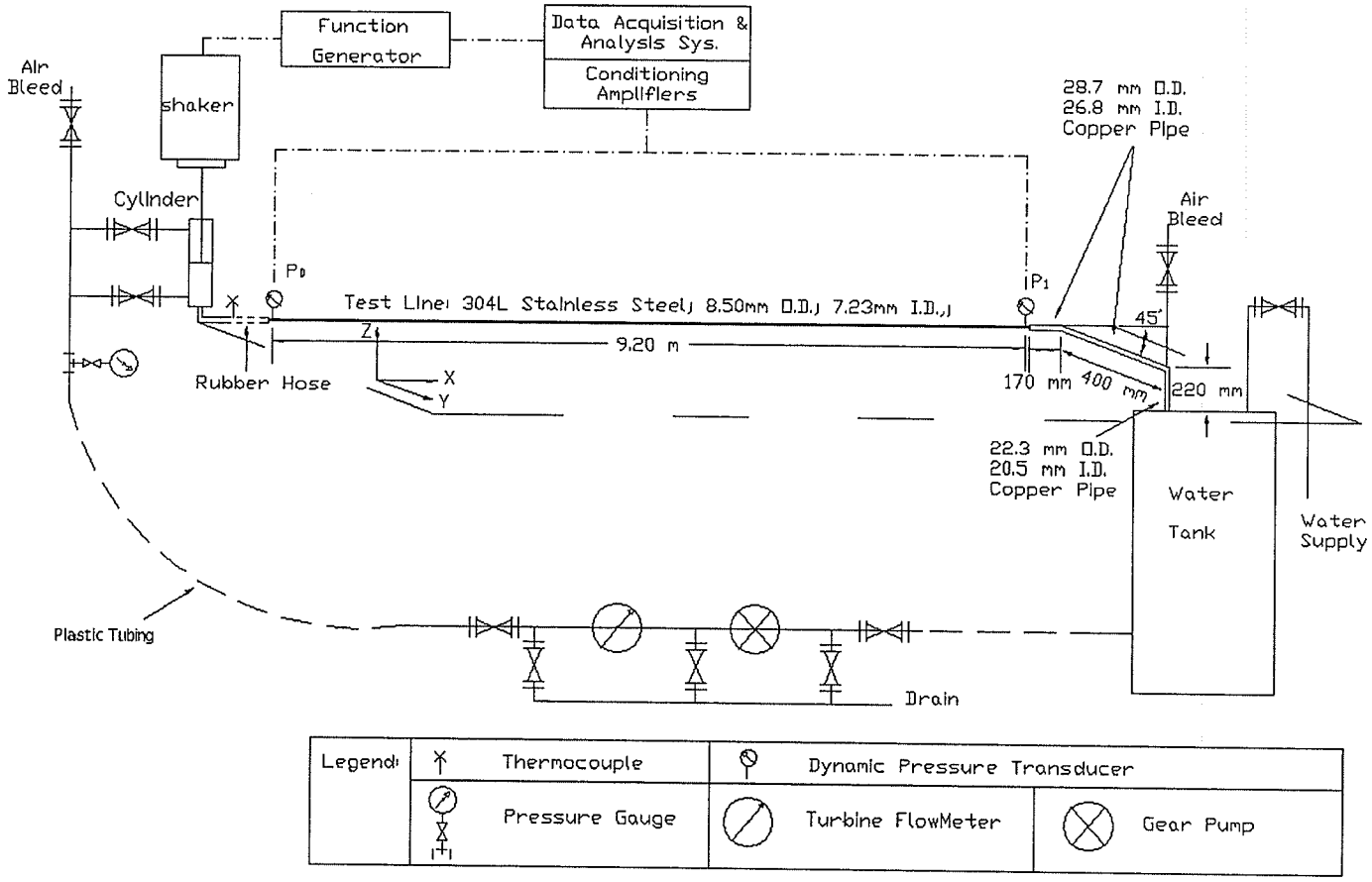

Figure 2: Schematic Diagram of The '9.20 m Turbulent Experiment' and '9.20 m 0-Flow Experiment' Setup

and the test lines to minimize the structure-born vibration from the cylinder and shaker.

2.1.3 Water-Feed Loop

Water was pumped by a Dynesco CJN Model gear pump from the city water system. Two plastic tubes were located at the upstream and downstream ends of the gear pump section to eliminate water hammer effects in the water-feed loop. A water tank stored water in the experiments of the 9.20 m test line.

2.1.4 Instrumentation

2.1.4.1 Shaker Control

A LDS PA100E-CE amplifier, an NI PCI-6731 high-speed analog output board, a function generating program 'Function Generator' (based on NI LabVIEW 7.1 system and shown in Figure 3) and a PC station were used to vary the amplitude and frequency of sine wave inputs to the shaker.

2.1.4.2 Data Conditioning and Acquisition System

The data conditioning and acquisition system consisted of a PCB model 482A16 charge amplifier, an NI PCI-4472 8-channel dynamic signal acquisition board, an 8-

channel data acquisition program 'DAQ-Test' (which is based on NI LabVIEW 7.1 system and shown in Figure 4), and a PC station.

2.1.4.3 Dynamic Pressure Measurement

Two PCB 112A22 model dynamic pressure transducers (dynamic pressure range: 0.01 — 50 psi, resolution: 0.001 psi, rise time: 2 μs) were located at upstream and downstream ends of each test line, and denoted as P_0 and P_1 respectively. Because the dynamic pressure transducers used in the experiments were new, on-field calibration was not performed. The calibration reports of pressure transducers are presented in Appendix D. They were flush-mounted on the pipe by a tee and a specially made transducer adaptor. The distance between the sensors and the center line of test lines was short enough (~4.5 cm) and could not distort the signals.

The signals from the dynamic pressure transducers were routed to the amplifier. The outputs from the charge amplifier were connected to the acquisition board, which stored the data for detailed post-processing. The program 'DAQ-Test' controlled the data acquisition, filtered noises and performed simple on-line analysis.

2.1.4.4 Static Pressure Measurement

A static pressure gauge was located at the upstream of the cylinder to measure the static pressure.

2.1.4.5 Temperature Measurement

A K-type thin thermocouple was inserted into the rubber hose to measure the water temperature. The thermocouple was connected to a thermometer.

2.1.4.6 Flow Rate Measurement

An OMEGA FTB-4607 model pulse-output turbine flow meter was located at the upstream of the gear pump to measure the steady flow rate. The pulse-output from the flow meter was connected to the acquisition board, and the pulse rate from the flow meter was obtained by the total harmonic distortion analysis (THD) in program 'DAQ-Test'. The flow rate was obtained by multiplying the pulse rate with a flow rate constant (75.7 Pulses per U.S. Gallon/Minute) supplied by the manufacturer.

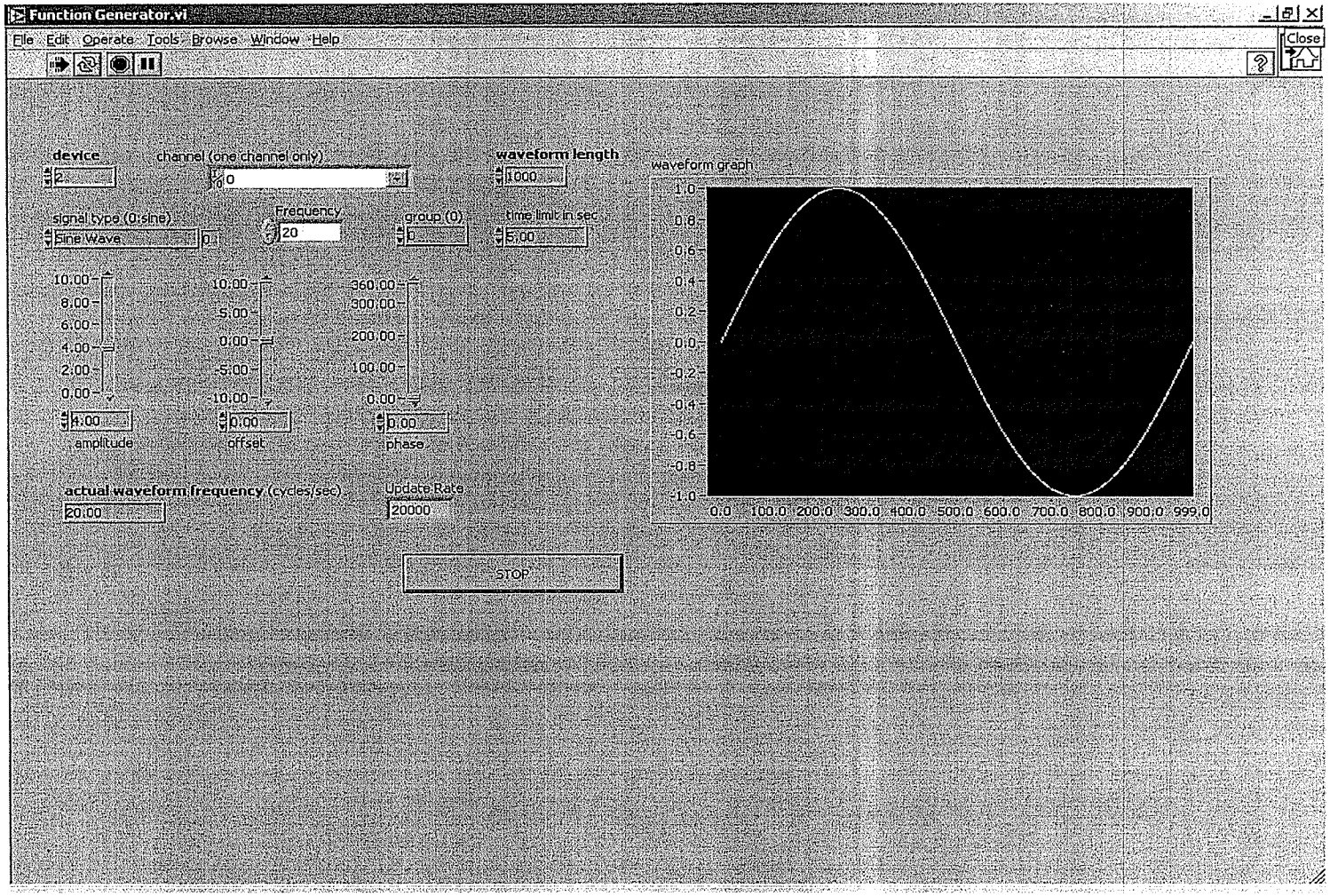

Figure 3: The Function Generating Program 'Function Generator'

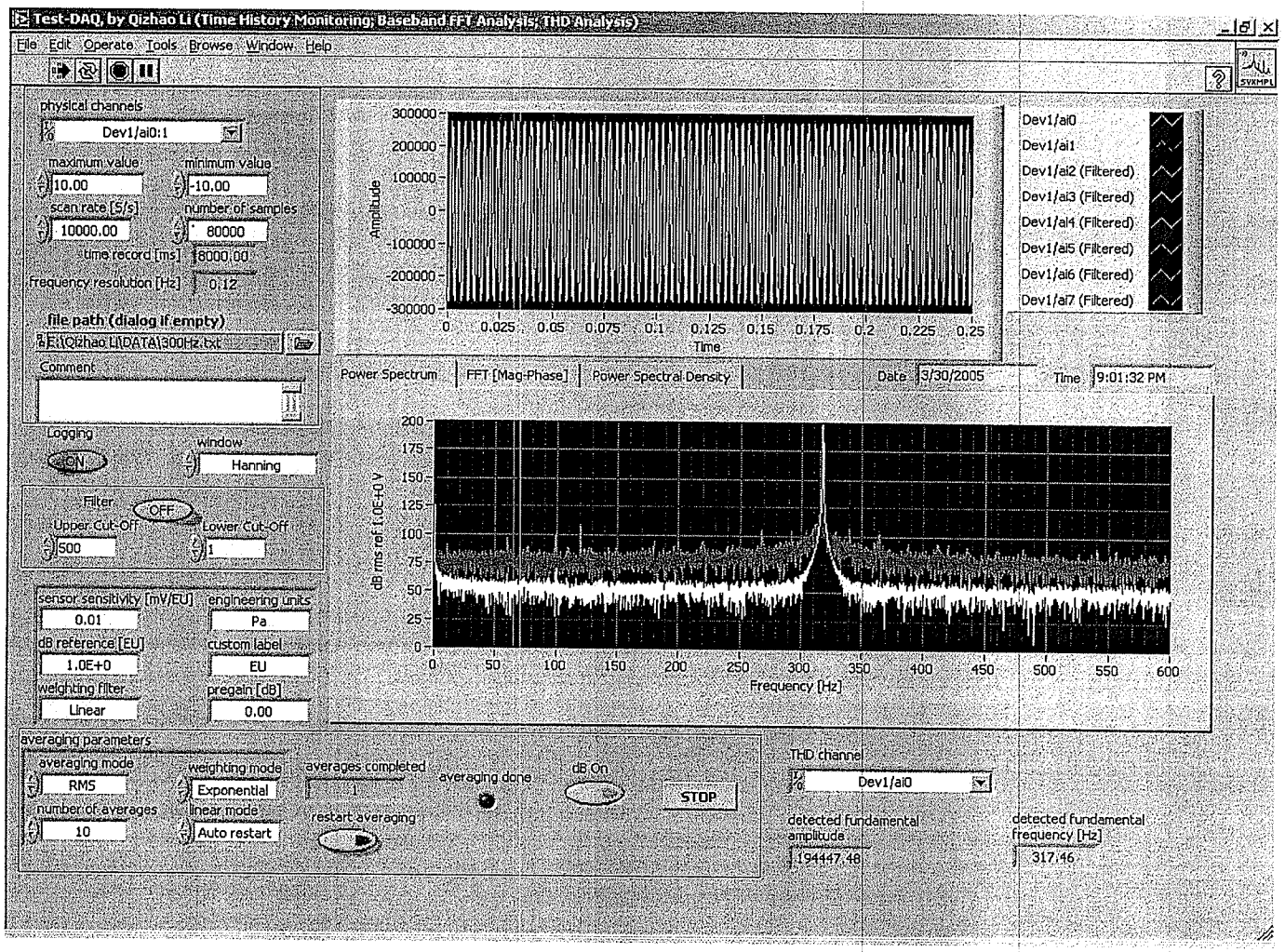

Figure 4: The 8-Channel Data Acquisition Program 'DAQ-Test'

2.2 Experimental Procedure

2.2.1 Air Bubbles Venting

The characteristic of frequency response in pipe flow can be largely affected if air bubbles are contained in the liquid. An obvious consequence is the sound speed in the liquid test line would be greatly reduced by air bubbles, even with a very small amount of air present. Figure 5 [87] illustrates the effect of air bubbles on the sound speed. To prevent the existence of air bubbles in the test line, before commencing each test, the test line was filled with water, pressurized and carefully vented to remove trapped air.

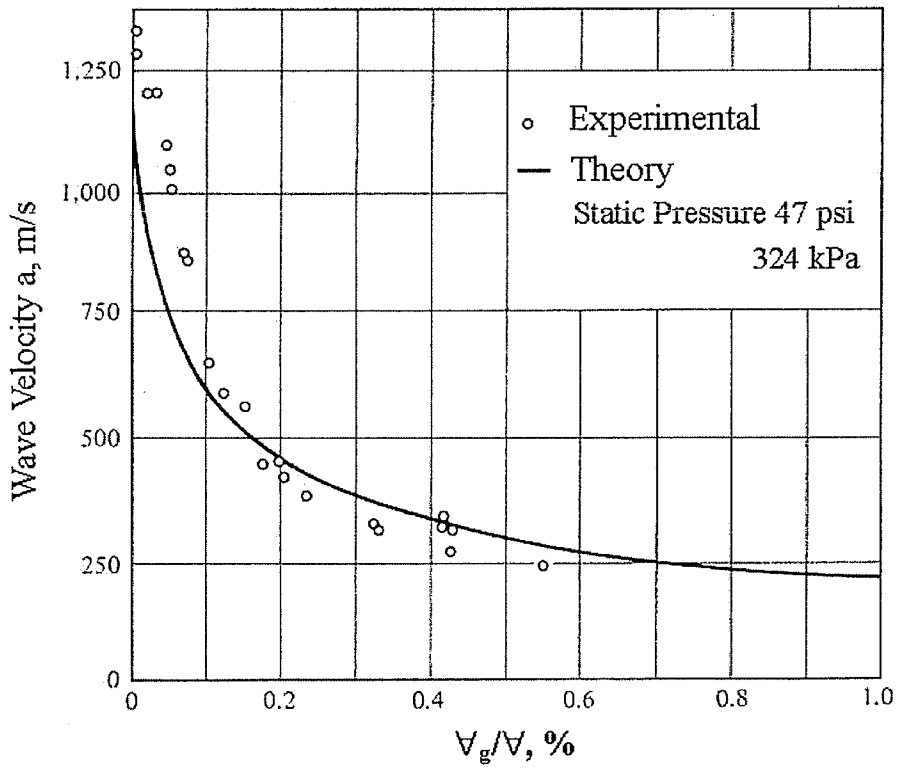

Figure 5: Propagation Velocity of A Pressure Wave in Pipeline for Varying Air Content (Theoretical and Experimental Results; ∀g — Gas Volume, ∀ — Total Volume) [87]

2.2.2 System Pressure Control

After air bubbles were vented, all the equipment was turned on. The system pressure was increased (or decreased) by increasing (or decreasing) the opening of the tap water valve.

2.2.3 Flow Rate Control

In the turbulent flow experiment, the flow velocity was adjusted by the gear pump.

2.2.4 Sound Speed Measurement

To check the existence of air bubbles, the sound speed of water was measured before each experiment. Because the volume of air bubbles is sensitive to system pressure, the sound speed of water containing air can be changed largely by the volume change of air bubbles under different system pressure, while the sound speed in pure water is not sensitive to the system pressure. The sound speed was measured under two system pressures, 0.2MPa and 0.5MPa, as a check of the air content in the line.

These sound speeds were compared with each other and with the theoretical sound speed. The theoretical sound speed is calculated by the following equation:

$$c = \sqrt{\frac{K/\rho}{1+\left(K/E\right)\left(2r/(R-r)\right)}} \qquad (1)$$

If the difference between the two measured sound speeds, or the differences between the measured sound speeds and theoretical sound speed, was large, it was believed that air bubbles were trapped in the fluid line. The venting procedure was repeated until air bubbles were vented.

In the measurement of sound speed, a single sine wave pressure pulse of 0.01 second period was produced by the shaker. The response time between the dynamic pressure transducers was measured. The speed of sound was obtained by dividing the distance between transducers by the response time.

Table 2 shows the speed of sound measured in each experiment and the theoretical speed of sound. It can be found that the differences between measured speeds of sound under different system pressure are small, and the measured speeds of sound agree well with the calculated. It illustrates that no air was trapped in test line during each experiment.

Table 2: Comparison between Measured Speeds of Sound and Theoretic Speeds of Sound

Experiment	7.03 m Dead-End (7.23 mm I.D., 8.50 mm O.D., T= 3.90 °C)	9.20 m Turbulence (7.23 mm I.D., 8.50 mm O.D., T= 3.90 °C)	9.20 m 0-Flow (7.23 mm I.D., 8.50 mm O.D., T= 7.22 °C)
Measured Sound Speed Under 0.5MPa System Pressure (m/s)	1358.74	1363.19	1388.86
Measured Sound Speed Under 0.2MPa System Pressure (m/s)	1365.87	1366.18	1377.96
Theoretical Sound Speed (m/s)	1346.34	1346.34	1358.48

2.2.5 Pressure Waves Control

During each test, the frequency of the pressure waves was incremented manually and held constant until the dynamic pressure stabilized. The frequency increments were 2 Hz for the off-resonance regions and 0.25 Hz through the resonance peaks (it was found adequate for accurate measurements). When changing the frequency, the shaker worked continuously to avoid possible changes in the period of changing frequency.

2.2.6 Data Collection

Data collection started approximately 30 seconds after the frequency change to exclude the effects of the previous frequency experiment.

According to the Nyquist theorem, the sampling rate should be at least twice the maximum frequency of interest. In practice, ten times of the Nyquist frequency are preferred for the sampling rate [88]. In this work, the interested frequency range is from 2 to 500 Hz. Hence, the sampling rate of dynamic pressures was set at 10,000 Samples/Second in each experiment. And to meet the requirement of frequency resolution of 0.25Hz in the post processing, 8 seconds (80,000 samples) were recorded in each experiment. This was deemed to be adequate.

The static fluid pressure was hand-logged every hour. The water temperature was hand-logged every hour.

2.2.7 Data Processing

In processing the data, a Fast Fourier Transform (FFT) analysis program called 'Analysis-FFT' did FFT calculation in the frequency domain. This is based on the NI LabVIEW 7.1 system and is shown as Figure 6. The amplitude of the dynamic pressures was obtained independently by FFT analysis from the time history of dynamic pressures. As a result, the pressure amplification at a given point on the test lines was obtained by dividing the downstream dynamic amplitude P_1 by the upstream dynamic amplitude P_0.

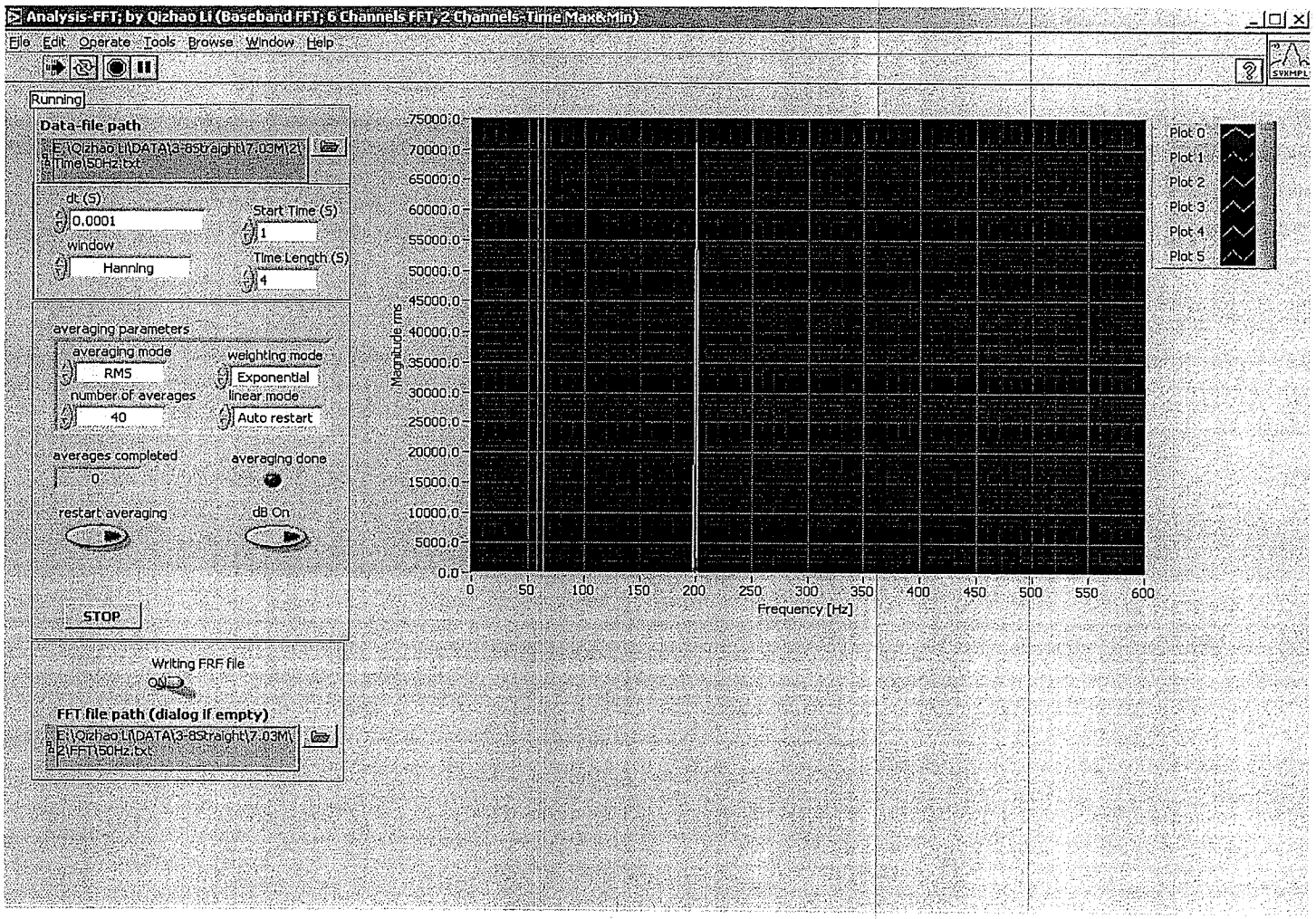

Figure 6: FFT Analysis Program 'Analysis-FFT'

CHAPTER THREE: Experimental Results and Discussion

3.0 Introduction

To investigate the characteristics of frequency response in both laminar and turbulent pipe flow, three experiments are performed in single straight test lines in laminar and turbulent flow in the frequency range of 2-500 Hz.

First, the frequency response of a dead-end test line (7.03 m length) was measured and the results were compared with the theoretic results of the transfer function method. The boundary condition at the dead-end is $u'=0$. This experiment is named '7.03 m dead-end experiment'. Second, to investigate the frequency response in turbulence flow, the frequency responses of a test line (9.20 m length) at a turbulent Reynolds number of 11514.94 was measured. Because the size of water tank located at the downstream of the test line is much larger than the test line, the boundary condition is approximately $P'=0$ at the water tank inlet. This experiment is named '9.20 m turbulent experiment'. Finally, to compare with the results of the second experiment, the frequency responses of same test line and boundary condition as the second experiment, but flow rate is zero, was measured. This experiment is named '9.20 m 0-flow experiment'.

3.1 Experimental Results

Results of the '7.03 m dead-end experiment' are shown in Figure 7. Results of the '9.20 m turbulent experiment' are shown in Figure 8. Results of the '9.20 m 0-flow experiment' are shown in Figure 9. Table 3 summarizes the experimental conditions of the three experiments. Table 4 summarizes the resonant amplifications and frequencies in the three experiments. The measured experiment data are given in Appendix A, B and C for the '7.03 m dead-end experiment', '9.20 m turbulent experiment' and '9.20 m 0-flow experiment' respectively.

Table 3: Experiment Conditions

Experiment	7.03m Dead-End	9.20m Turbulence	9.20m 0-Flow
Test Line Length (m)	7.03	9.20	9.20
Test Line O.D. (mm)	8.50	8.50	8.50
Test Line I.D. (mm)	7.23	7.23	7.23
Fluid	Water	Water	Water
System Pressure (MPa)	0.4	0.2	0.2
Temperature Shift in The Experiment (°C (Frequency Range))	3.90 (2-174 Hz) 4.44 (176-242 Hz) 3.90 (244-500 Hz)	3.90 (2-100 Hz) 4.44 (102-200 Hz) 5.00 (202-500 Hz)	7.22 (2-250 Hz) 7.78 (252-500 Hz)
Flow Rate (m/s)	0	2.42	0
Reynolds Number	0	11,514.94	0

Table 4: Resonant Amplitudes and Frequencies

Experiment	7.03 m Dead End		9.20 m Turbulence		9.20 m 0-Flow	
	Freq. (Hz)	Amplification	Freq. (Hz)	Amplification	Freq. (Hz)	Amplification
1	46.50	26.75	36.00	0.0371	37.00	0.1151
2	147.50	22.44	72.75	1.1066	75.00	1.6708
3	250.00	18.51	152.00	3.6140	153.75	1.9300
4	352.00	12.90	221.25	2.4755	230.00	5.0113
5	452.75	10.39	294.25	1.5732	304.00	11.0382
6			376.25	1.2033	381.75	9.6277
7			448.00	0.8072	461.00	4.8477

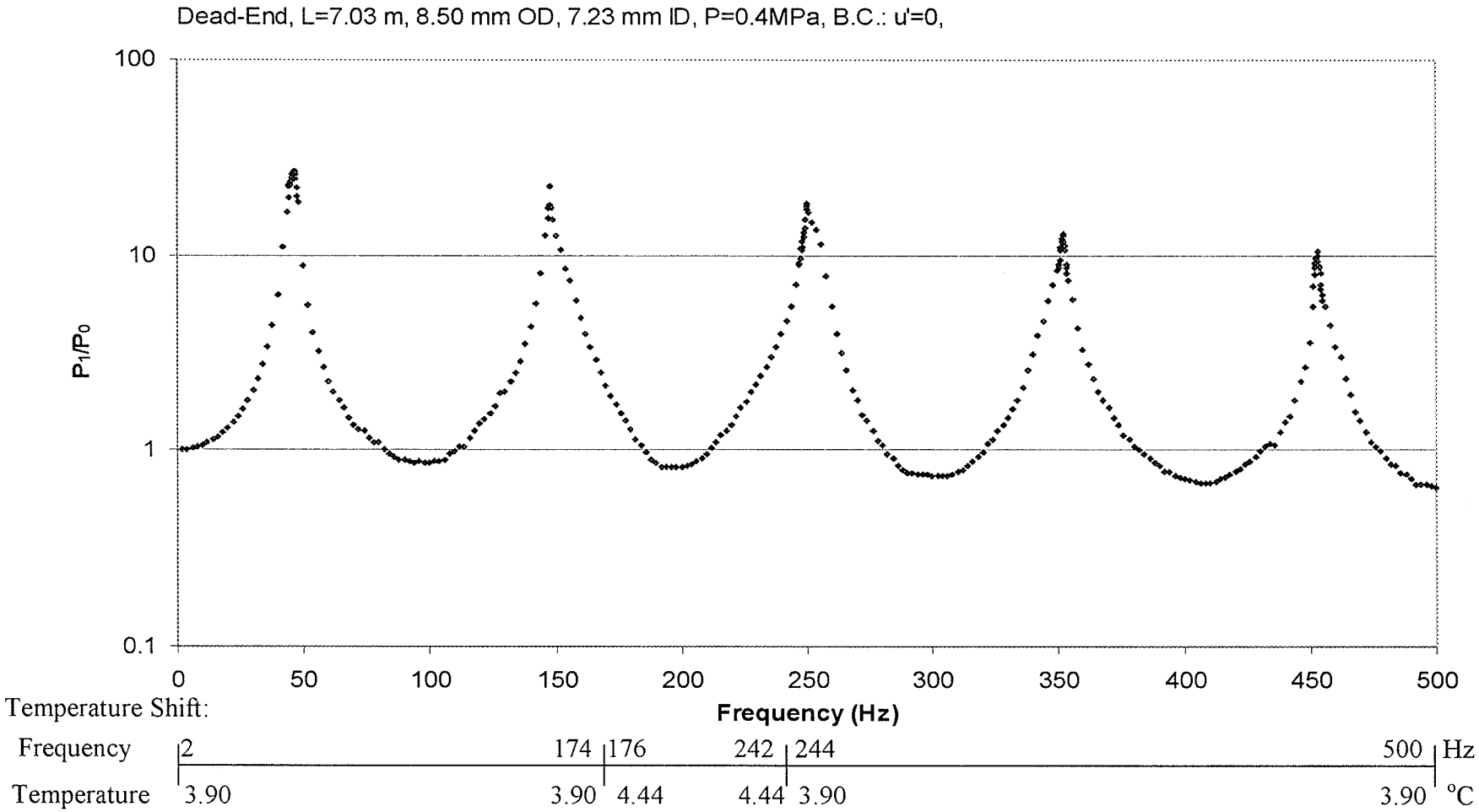

Figure 7: Results of The '7.03 m Dead-End Experiment'

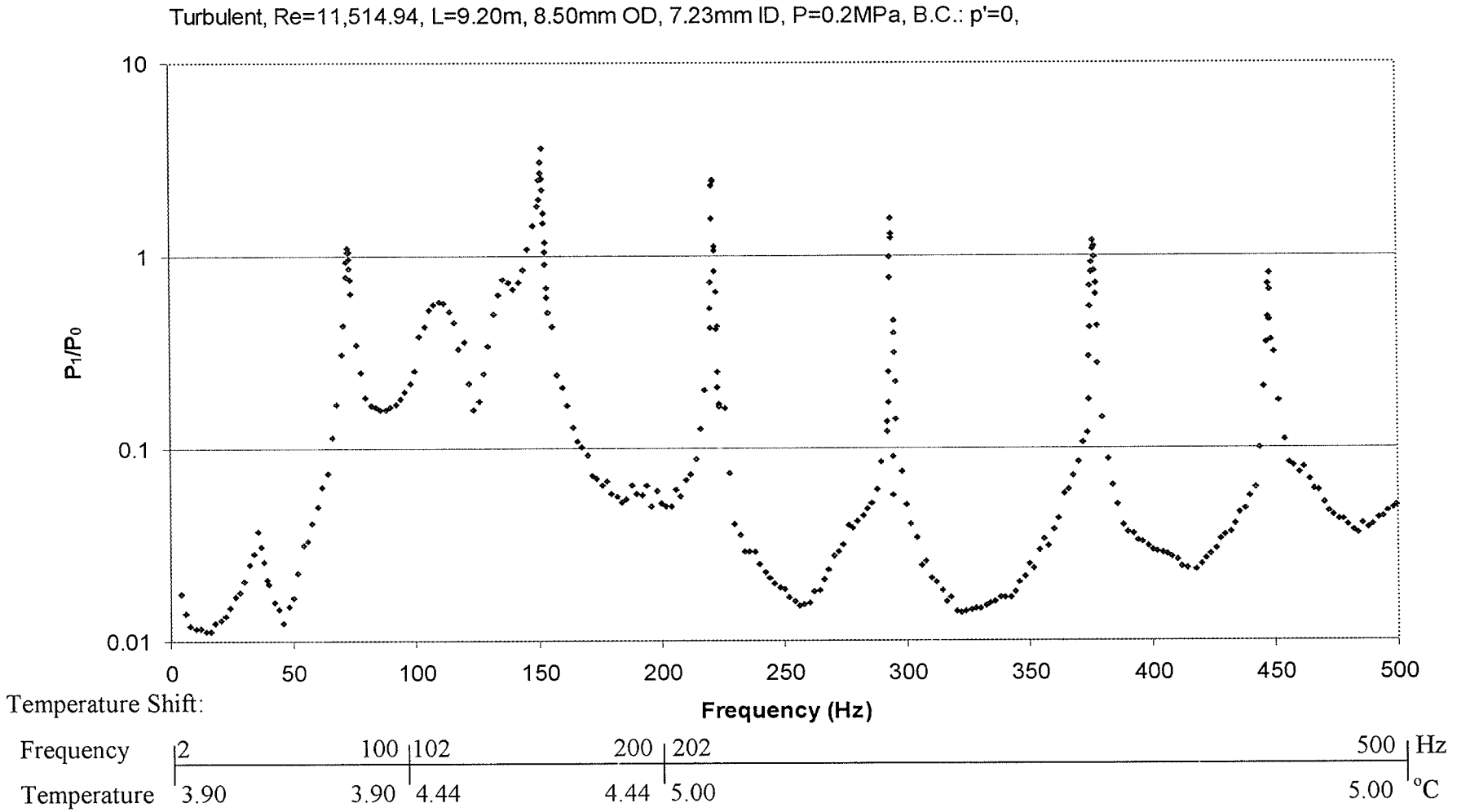

Figure 8: Results of The '9.20 m Turbulent Experiment'

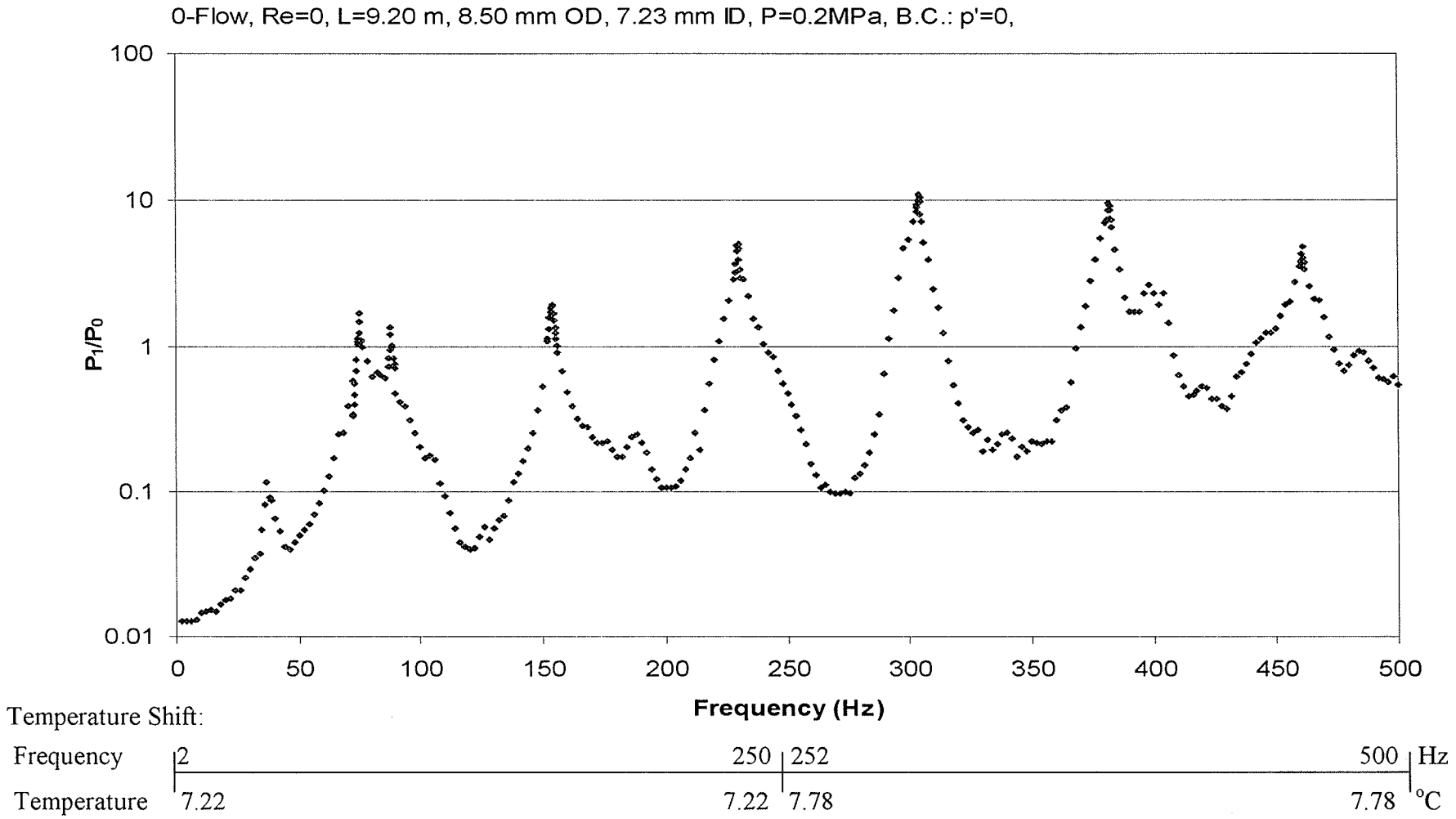

Figure 9: Results of The '9.20 m 0-Flow Experiment'

3.2 Discussion of Results

3.2.1 The '7.03 m Dead-End Experiment' Results

From the frequency response of the 7.03 m dead-end line shown in Figure 7, it can be seen that:

(1) The resonant amplifications decrease with the increasing in the resonant frequencies.

(2) In the no-resonance region, the minimum amplifications decrease with the increasing frequency.

(3) It can be found that the resonance frequencies can be reasonably well predicted by the 'organ-pipe' equation, $f_R=(2n-1)c/4L$ where f_R is the resonant frequency and n=1,2,3....

3.2.2 The Results of The '9.20 m Turbulent Experiment' and The '9.20 m 0-Flow Experiment'

The setups of '9.20m turbulent experiment' and '9.20m 0-flow experiment' were identical, and the experiment conditions were close, except the flow rate. Therefore, it is meaningful to compare the results of two experiments. Figure 10 shows the comparison between the results of the '9.20 m turbulent experiment' and the '9.20 m 0-flow experiment'.

As shown in Figure 2, the pipe diameter increased right after the downstream transducer P_1, and the transducer P_1 was close to the water tank. The dynamic pressures at the downstream end were much lower than the pressures at upstream end, because the energy of acoustic waves was mainly absorbed by the water tank. Therefore, the amplifications were low in both the '9.20 m turbulent experiment' and the '9.20 m 0-flow experiment'.

It is found that as frequency increased, the amplifications of the '9.20 m 0-flow experiment' become larger than the amplifications of the '9.20 m turbulent experiment'. This is because the damping is much larger in turbulent flow than in laminar flow. And the resonant regions in turbulent flow are narrower than the resonant regions in 0-flow. It is important to note this.

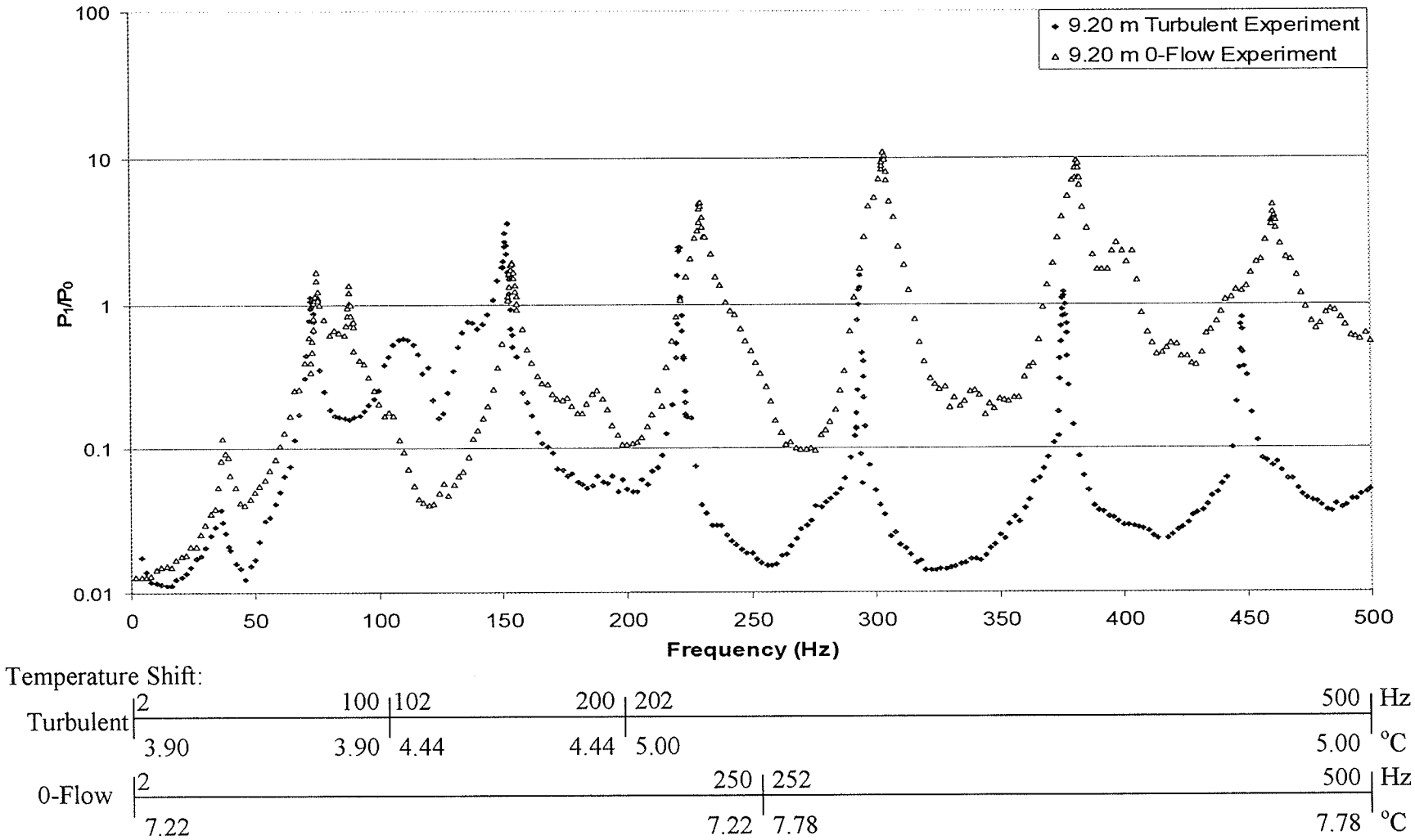

Figure 10: Comparison between Results of 9.20m Turbulent and 9.20m 0-Flow Experiments

3.3 Possible Experimental Errors

In the experiments, several factors can affect the accuracy of the results. They are instruments uncertainties, vibration, shaker noise, and oscillating pressures generated by gear pump in the 9.20m turbulent experiment.

3.3.1 Instruments Uncertainties

The uncertainties of instruments are listed in Table 5. Because the PCB 482A16 charge amplifier, the NI PCI-4472 signal acquisition board, and the NI PCI-6731 analog output board were not calibrated by the manufacturers, the systematic uncertainty of the measurement system is not be calculated.

Table 5: Instruments Uncertainties

Instrument	Uncertainty
PCB 112A22 Dynamic Pressure Transducer	0.64%
OMEGA FTB-4607 Turbine Flow Meter	1.5%

3.3.2 Effects of Vibration

By fixing test lines at every 25 cm by cushioned clamps and locating a short rubber hose between the test line and cylinder, the natural frequency of longitudinal vibrations of test lines was much above the experimental frequency range. By

especially fixing the line ends, axial vibration was reduced to be as small as possible. Since no vibration sensors were mounted, the effect of vibration would not be estimated.

3.3.3 Effects of Shaker Noises

During the experiments, the electromechanical shaker produced noise and the noise increased with frequency. Because the dynamic pressure transducers are sensitive, it can affect the transducers signals, especially the upstream transducer P_0 which was located only 0.8 m far away from the shaker. By disconnecting the shaker and cylinder, the effects of shake noise on the transducers were measured under the condition of the '7.03 m dead-end experiment' at the highest frequency 500 Hz. This is shown in Figure 11. It can be seen that the largest amplitude of shaker noise is located in low frequencies which were filtered by the data acquisition system. And the largest amplitude at 500 Hz was only 0.6 Pa, much smaller than the dynamic pressure signals which were larger than 100 Pa. Therefore, the effects of shaker noise on pressure transducers were small enough and would not produce large errors.

3.3.4 Effects of Gear Pump in The '9.20 m Turbulent Experiment'

In the '9.20 m turbulent experiment', a gear pump was used to drive water through the loop. As is well known, pump can produce pressure pulsations at the vane-passing frequency. The pump-generated pressure pulsations were measured before the experiment, shown in Figure 12. It can be found that the vane-passing frequency was

only 3.5 Hz, much lower than the natural resonant frequency of the test line. It can not produce resonant vibration. Also it is not in the interested frequency range (50 — 500 Hz). The effects of gear pump were small and would not produce large errors.

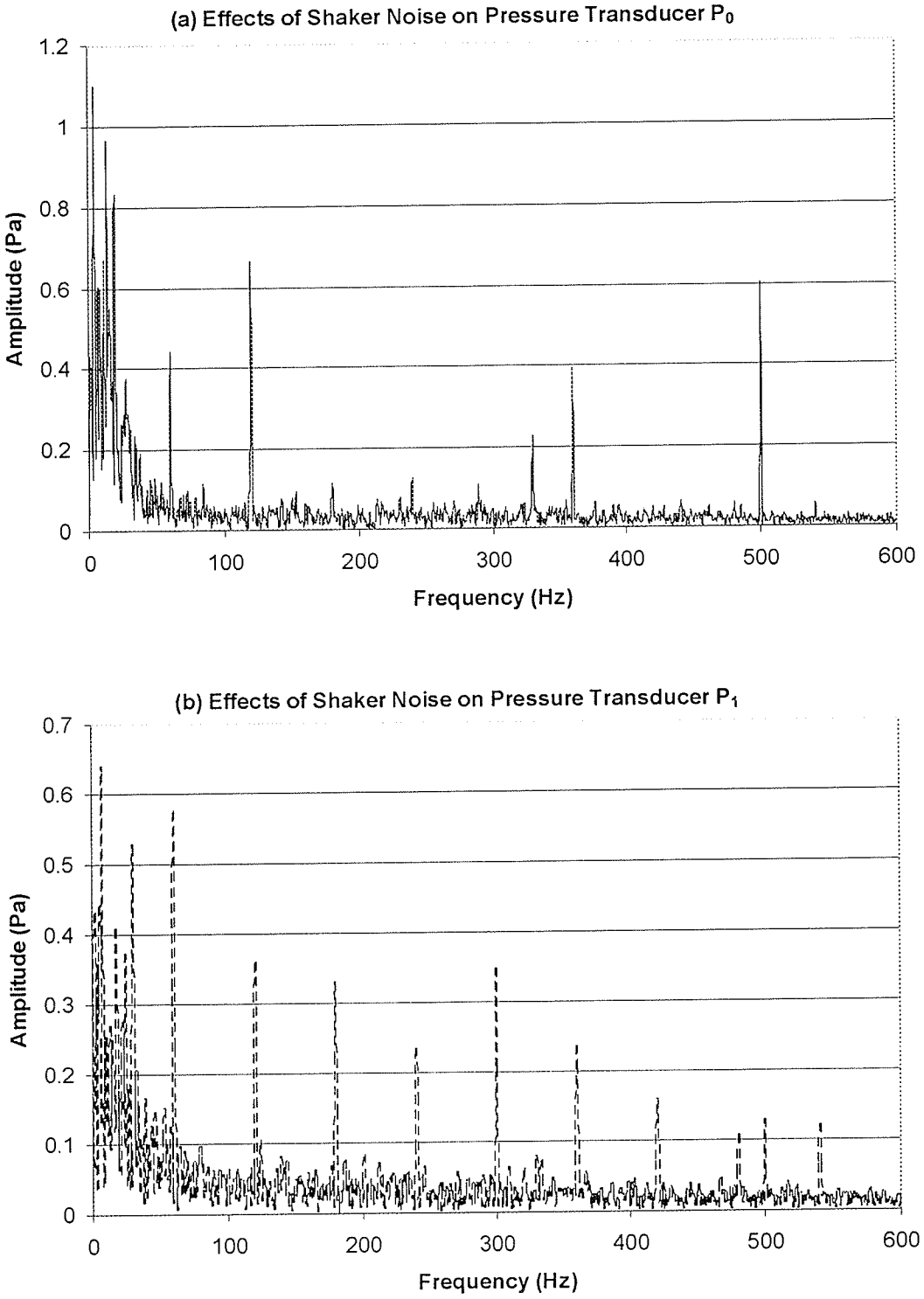

Figure 11: Effects of Shaker Noise on Pressure Transducers

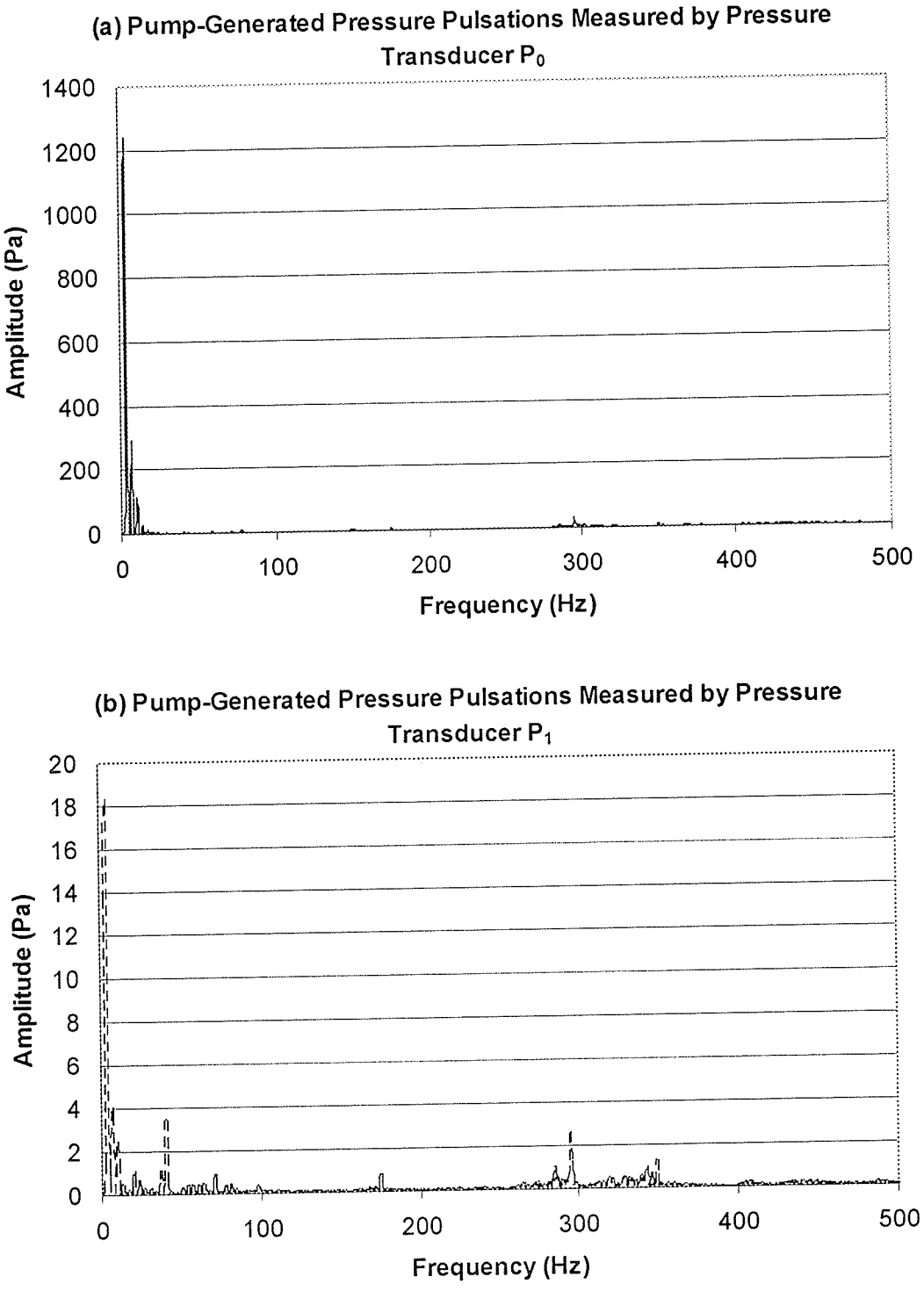

Figure 12: Pressure Pulsations Generated by Gear Pump

CHAPTER FOUR: Analysis of The Experimental Results

4.1 Comparison between Results of The '7.03 m Dead-End Experiment' and Transfer Function Models

A simple transfer function [84] for the dead-end line (boundary condition: u'=0 at the dead-end), shown in following, is calculated.

$$\frac{P_1(s)}{P_0(s)} = \frac{1}{\cosh\Gamma(s) + \frac{R_P}{Z(s)}\sinh\Gamma(s)} \tag{2}$$

where,

$$\Gamma(s) = s\frac{L}{c}\left[1 - \frac{2J_1(jz)}{jzJ_0(jz)}\right]^{-\frac{1}{2}} \tag{3}$$

$$Z(s) = \frac{\rho c}{\pi r^2}\left[1 - \frac{2J_1(jz)}{jzJ_0(jz)}\right]^{-\frac{1}{2}} \tag{4}$$

$$z = r\sqrt{s/\upsilon} \tag{5}$$

$$R_P = \zeta\frac{\rho}{\pi r^3}\sqrt{2\upsilon w} \tag{6}$$

$$s=jw \tag{7}$$

The solutions of the transfer function for 7.03 m dead-end test line with both the measured and theoretic speed of sound were calculated, and compared with the results of the '7.03 m dead-end experiment'. The empirical constants used in the model are summarized in Table 6. The comparison is shown in Figure 13. The

resonance amplifications and frequencies of theory and experiment are shown in Table 7. In addition, for resonance frequencies, the theoretic result by using measured speed of sound has better agreement with the experimental results than the result by using calculated speed of sound. Both solutions of the transfer function can predict the resonance amplifications.

Table 6: Empirical Constants Used in Transfer Functions

Constant	Symbol	Value	Unit
Water Viscosity	υ	1.5717 (2-174 Hz)	$Pa.S\times10^{-6}$
		1.5448 (176-242 Hz)	
		1.5717 (244-500 Hz)	
Water Density	ρ	1000.1 (2-174 Hz)	Kg/m^3
		1000.1 (176-242 Hz)	
		1000.1 (244-500 Hz)	
Line Young's Modulus of Elasticity	E	200	GPa
Line Poisson's Ratio	ν	0.29	--
Water Bulk Modulus of Elasticity	K	2.0214 (2-174 Hz)	GPa
		2.0283 (176-242 Hz)	
		2.0214 (244-500 Hz)	
Resistance Coefficient for Line Elements	ζ	0.1 [84]	--

Table 7: Resonance Amplification and Frequencies for the 7.03m Dead-End Test Line

	Experiment Results		Theory with Measured Speed of Sound		Theory with Theoretic Speed of Sound	
	Freq. (Hz)	Amplification	Freq. (Hz)	Amplification	Freq. (Hz)	Amplification
1	46.50	26.75	48.00	40.91	47.00	42.80
2	147.50	22.44	144.00	24.73	142.00	24.94
3	250.00	18.51	240.00	17.54	237.00	19.36
4	337.00	12.25	338.00	15.61	332.00	16.30
5	438.50	10.36	434.00	14.50	427.00	14.23

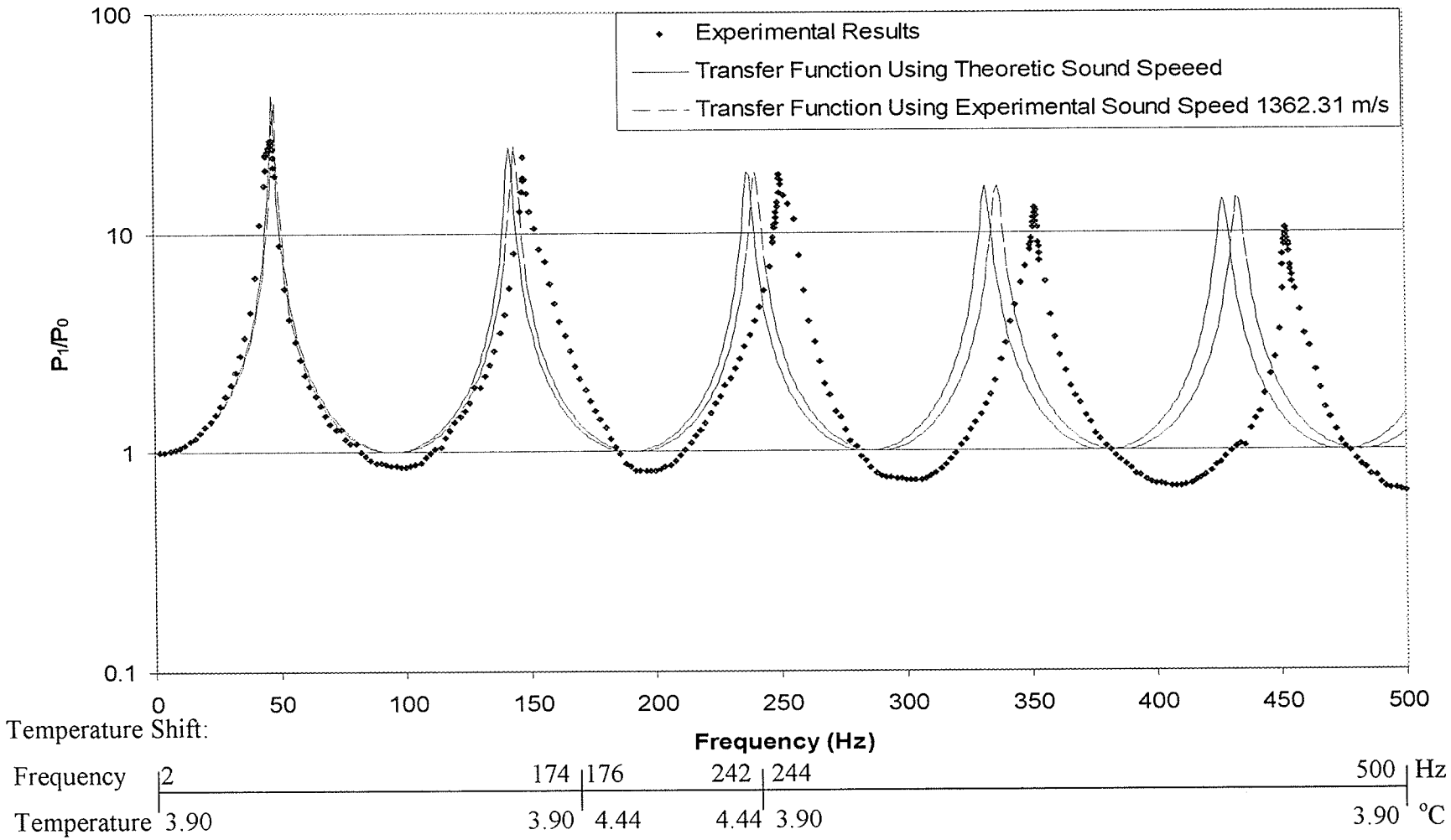

Figure 13: Comparison between Results of The '7.03m Dead-End Experiment' and Transfer Functions

Comparing the experiment results with theoretic results, three phenomena can be found:

(A) In the no-resonance region, the minimum amplifications are lower than the theoretic prediction, which is unity. This result was also obtained by Rzentkowski [84], shown in Figure 15. This is believed to be caused by the effects of frequency-dependent damping and reflected acoustic waves. As shown in Figure 14, by the linear least squares fitting method, the minimum amplifications in the no-resonance area can be fitted with a straight line, given by:

$$Min(P_1 / P_0) = -0.0006 f_M + 0.9202 \tag{8}$$

A similar slope is found in Rzentkowski's experiments, formulated as:

$$Min(P_1 / P_0) = -0.0008 f_M + 0.9167 \tag{9}$$

These two slopes are reasonably close.

(B) As shown in Figure 14, a straight line can be found for resonance amplifications decreasing with frequency, given by:

$$Max(P_1 / P_0) = -0.0416 f_R + 28.5786 \tag{10}$$

A similar slope found in Rzentkowski's experiment is formulated as:

$$Max(P_1 / P_0) = -0.0458 f_R + 25.4616 \tag{11}$$

These two slopes have good agreement.

(C) The resonant frequencies shift linearly as frequency increasing, shown in Figure 16. Comparing with transfer function using theoretic sound speed, the resonant

frequency shifts can be formulated as:

$$\Delta f = 0.0659 f_R - 3.7055 \quad (12)$$

And comparing with transfer function using measured sound speed, the resonant frequency shifts can be formulated as:

$$\Delta f = 0.0531 f_R - 3.9126 \quad (13)$$

This phenomenon also can be found in Rzentkowski's experiments after the first resonance, shown in Figure 17. Comparing with transfer function using theoretic sound speed, the resonant frequency shifts found in Rzentkowski's experiments can be fitted by:

$$\Delta f = 0.0448 f_R - 10.8360 \quad (14)$$

Comparing with transfer function using measured sound speed, the resonant frequency shifts found in Rzentkowski's experiments can be fitted by:

$$\Delta f = 0.0502 f_R - 10.7754 \quad (15)$$

The formulae of the resonant frequency shifts found in the '7.03m dead-end experiment' and Rzentkowski's experiments are in good agreement.

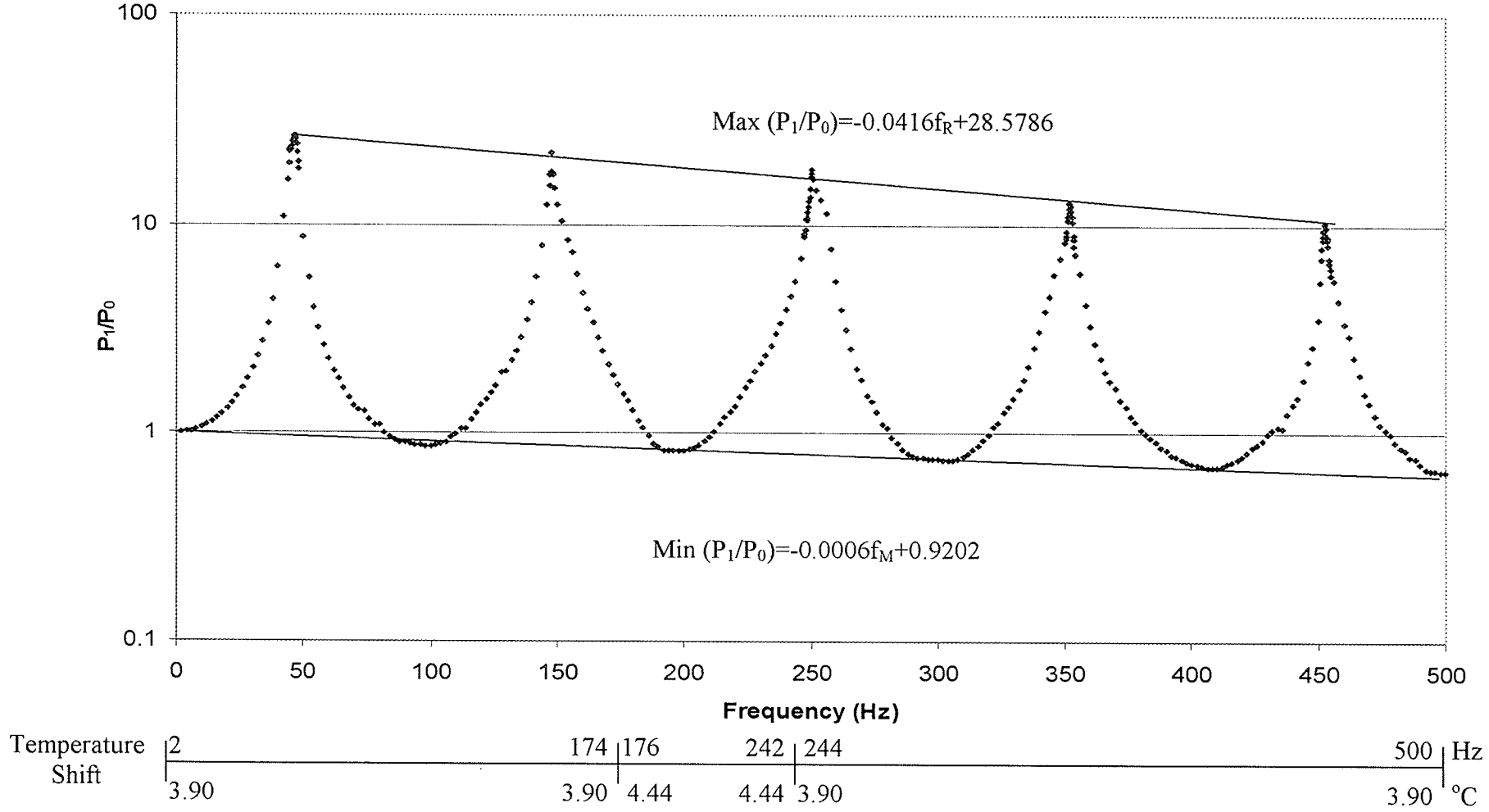

Figure 14: Slopes of Resonance Amplifications and Minimum No-Resonance Amplifications in 7.03m Dead-End Experiment

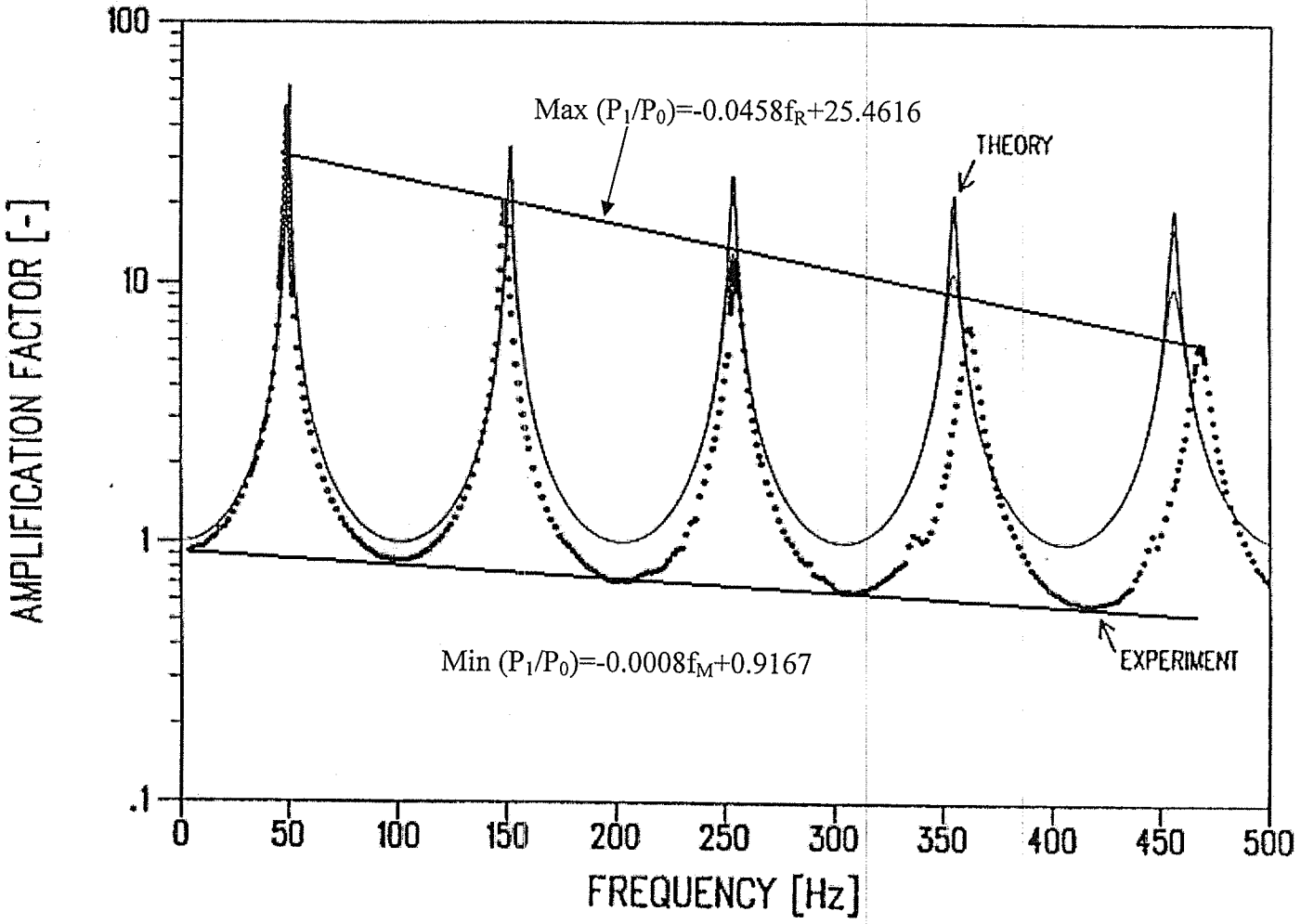

Figure 15: Slopes of Resonance Amplifications and Minimum Amplifications in Rzentkowski's Experiment [84]

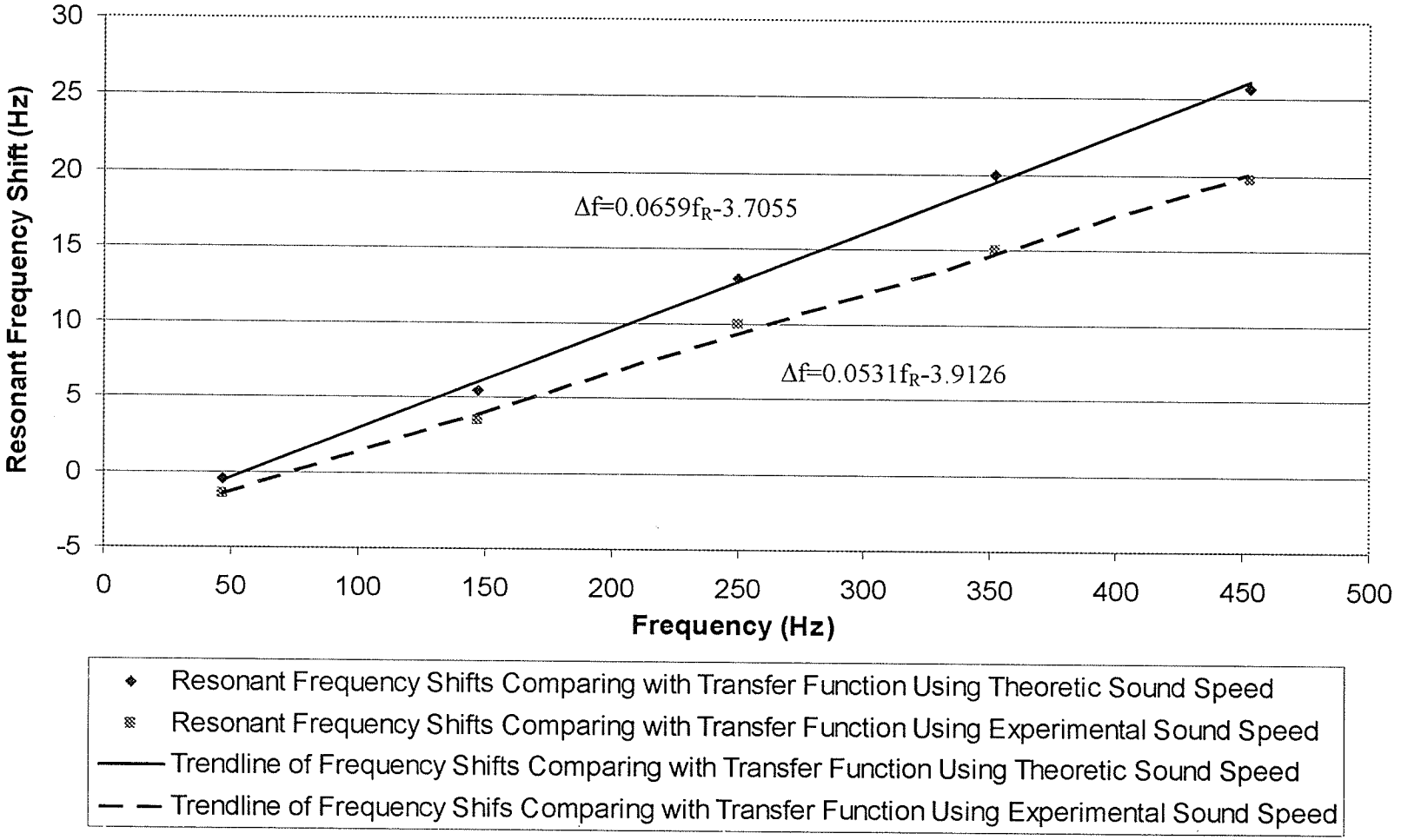

Figure 16: Resonant Frequency Shifts in The '7.03 m Dead-End Experiment'

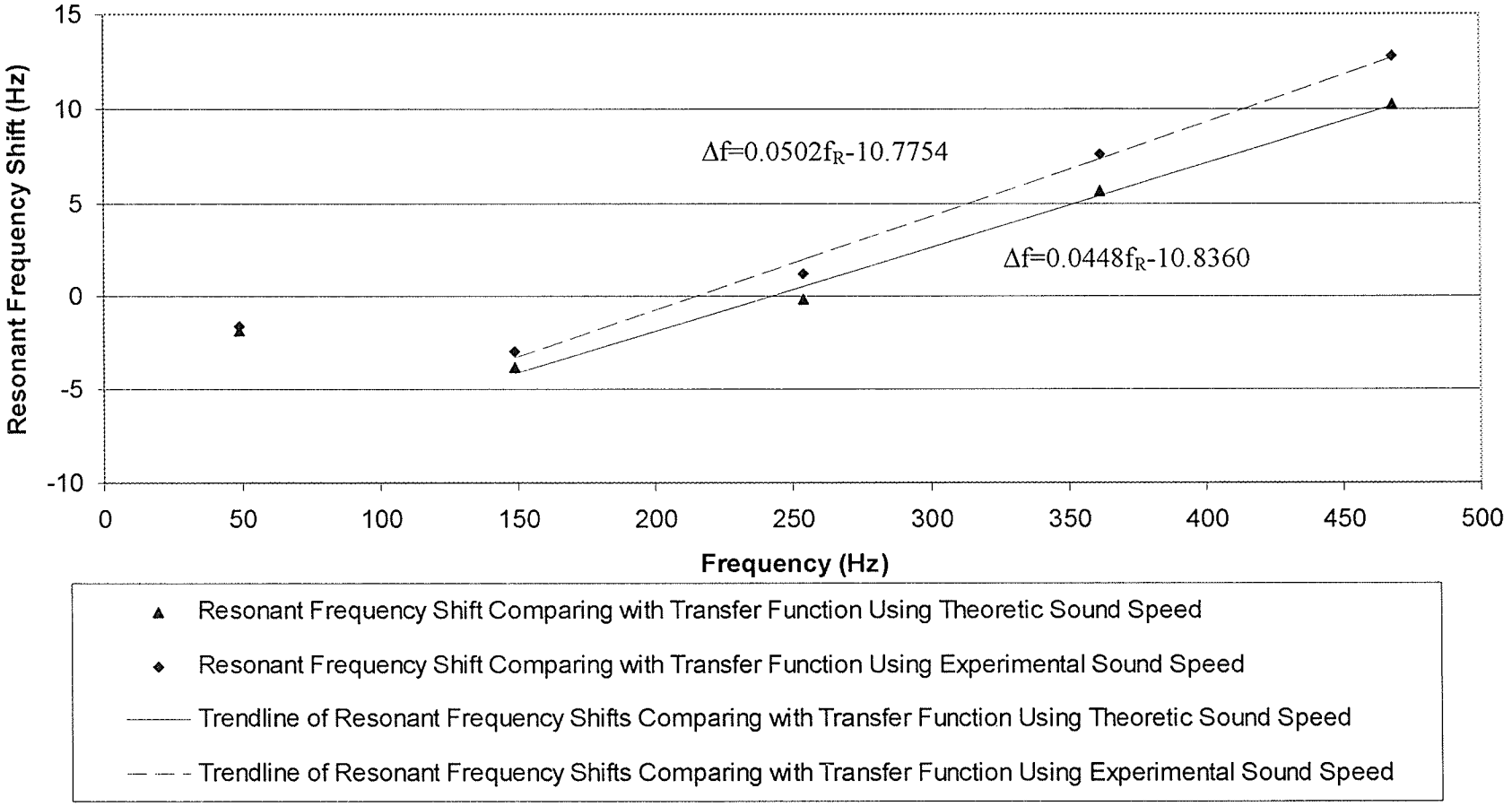

Figure 17: Resonant Frequency Shifts in Rzentkowski's Experiments

4.2 Analysis of The '9.20m Turbulent' and '0-Flow' Experiments Results

Similar with the slope for resonance amplifications found in the '7.03m dead-end experiment', a slope fitting resonance amplification can be found in the '9.20m turbulent experiment' after the second resonance, shown in Figure 18. The slope can be formulated as:

$$Max(P_1 / P_0) = -0.0092 f_R + 4.6685 \qquad (16)$$

As previously mentioned, the resonant peaks in the '9.20 m turbulent experiment' result are sharper than the resonant peaks in the '9.20 m 0-flow experiment' result. The resonant peak widths at 2/3 peak amplitude are calculated and listed in Table 8. It can be found that, the band width of the first two resonant peaks in turbulent experiment is larger than the band width of the first two resonant peaks in 0-flow experiment. With frequency increasing, after the third resonant peak, the band width of the resonant peaks in turbulent experiment becomes less than the band width of the resonant peaks in 0-flow experiment.

Table 8: Resonant Peak Widths of The '9.20m Turbulent' and '0-Flow' Experiments

		Resonant Peak No:						
		1st	2nd	3rd	4th	5th	6th	7th
Band Width at 2/3 Peak Amplitude (Hz)	0-Flow	3	1	2.75	1.75	3	3	2
	Turbulent	6	1.75	1	1	0.75	1.5	1

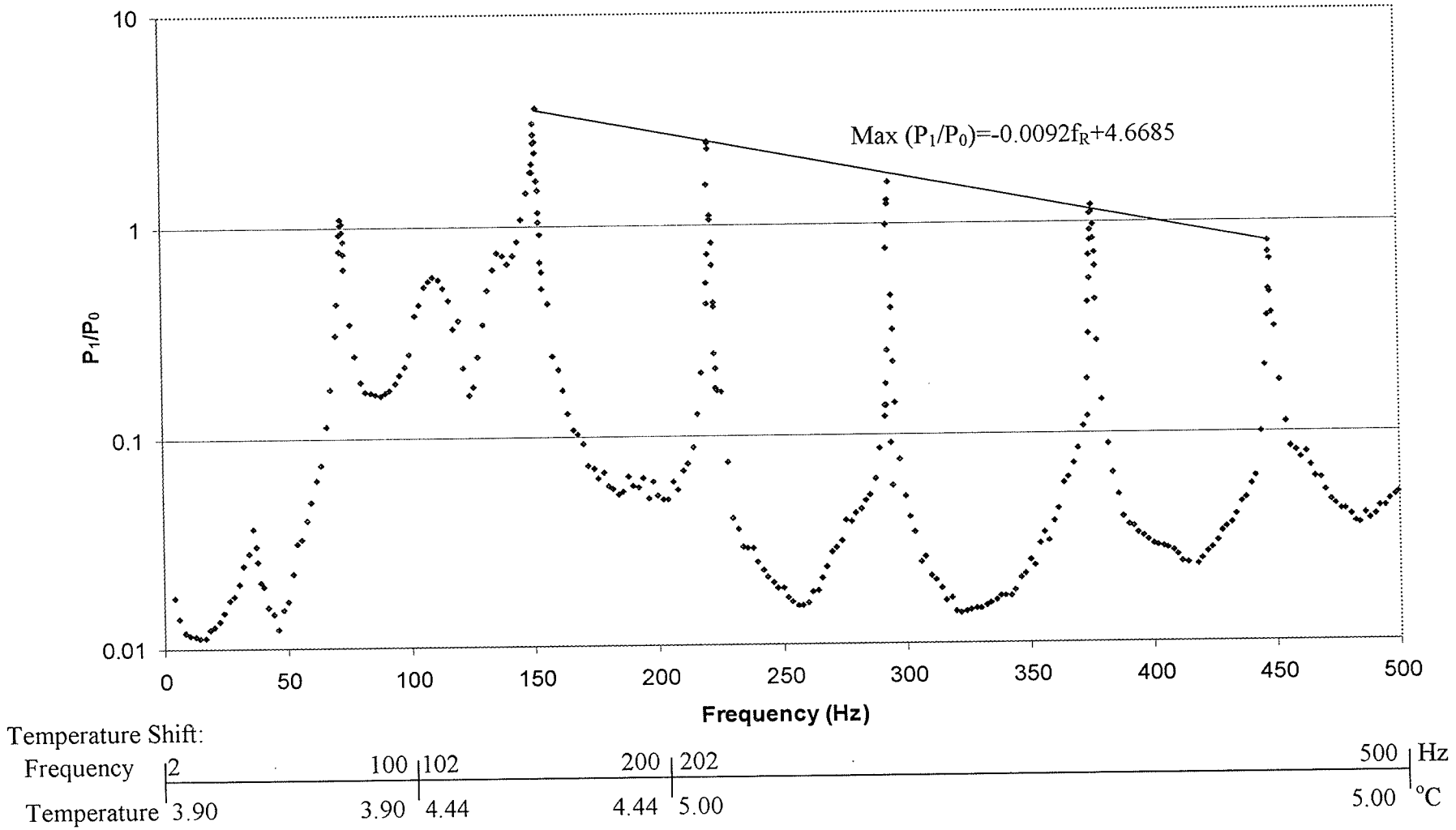

Figure 18: Slope for Resonance Amplifications in The '9.20 m Turbulent Experiment'

CHAPTER FIVE: Conclusions

Three frequency response experiments of test lines were presented. Possible experimental errors were discussed and the experiment accuracy was stated.

The result of the '7.03 m dead-end experiment' was compared with the solution of a simple transfer function and got a good agreement. The comparison revealed three phenomena:

(1) The minimum frequency responses of test line are damped by the effects of frequency-dependent friction, lower than unity which is the prediction of the theoretic model. The minimum amplifications decrease linearly as frequency increasing.

(2) The resonant amplifications decrease linearly with frequency increasing.

(3) Comparing with theoretic calculation, the resonant frequency shifts increase linearly with resonant frequency increasing.

The results of the '9.20 m turbulent experiment' and the '9.20 m 0-flow experiment' were compared and the waveforms were close. In the '9.20 m turbulent experiment', a slope also can be found for the resonant amplification reduction. The results were presented for further development of theoretic models.

CHAPTER FIX: Recommendations

In the experiments, the frequency control and data acquisition were performed in one PC station by software. Limited by the performance of the PC station, the frequency can not be adjusted accurately in high frequency range. More time was used on the frequency adjustment during the experiments. It made the experiments can not be performed automatically and finished in short time. One experiment has to be finished in several days, and it made water temperature varied. It is recommended that the frequency can be controlled by an independent PC station or a hardware function generator. Hence, the experiment can be performed automatically and finished fast.

Because in the open-end line experiments, the frequency responses between the inlet and 7.03 m at the test line were not measured, the results cannot compared with the result of the '7.03 m dead-end experiment'. The frequency responses between the inlet and 7.03 m at open-end test line are recommended to be measured, both in laminar and turbulent flows. Also frequency responses in bended lines and branch lines are recommended to be measured for further research.

References

[1] Martin, D., and Skears, J., "Darlington NGS Unit 3 Test Program", Ontario Hydro, DND report 92075, April 1992.

[2] Barreca, S. L., and Urbanowicz, J., "Darlington N12 Investigation Full-Scale Acoustic Tests of PHT piping Design solutions", OHRD Report, Nuclear Process Components Test Facility, Sep. 1992, 92-218-K

[3] Martin, D., and Pascoe, J., "Final Report on the Darlington NGS Unit 3 Test Program", Ontario Hydro, Report No. 931022, Oct. 1993

[4] Daily, W. L., Hankey, W. L., Olive, R. W., and Jordaan, J. M., "Resistance Coefficients for Accelerated and Decelerated Flows through Smooth Tubes and Orifices", Trans. ASME, Vol. 78, 1956, pp. 1071-1077

[5] Safwat, H.H., and Polder, J.V.D., "Friction—Frequency Dependence For Oscillatory Flows In Circular Pipe", J. of The Hydraulics Division, ASCE, Vol. 99, No. HY11, Nov. 1973

[6] Hino, M., Sawamoto, M., and Takasu, S., "Study on The Transition to Turbulence and Frictional Coefficient in An Oscillatory Pipe Flow", Transactions of JSCE, 1977, pp. 282-284

[7] Wood, F. M., "The Application of Heaviside's Operational Calculus to the Solution of Problems in Water Hammer", Trans. ASME, Vol. 59, 1937, pp. 707-713

[8] Rich, G. R., "Water-Hammer Analysis by the Laplace-Mellin Transformation", Trans. ASME, Vol. 67, 1945, pp. 361-376

[9] D'Souza and Oldenburger, R., "Dynamic Response of Fluid Lines", ASME Trans, J. of Basic Engng., Series D, Vol. 86, p. 589-598, 1964 September.

[10] Foster, K., and Parker, G.A., "Transmission of Power by Sinusoidal Wave Motion Through Hydraulic Oil in a Uniform Pipe", Procs, Instn. Mech. Eng., 179: Pt. 1 (19), p. 599-612, 1964-1965

[11] Brown, F.T., Margolis, D.L., and Shah, R.P., "Small-Amplitude Frequency Behavior of Fluid Lines with Turbulent Flow", J. of Basic Engineering, Trans. of the ASME, Dec. 1969, p. 678-692

[12] Philips, E.M., and Chiang, S.H., "Pulsatile Newtonian Frictional Losses in a Rigid Tube", Int. J. Engng Sci., 1973, Vol. 11, p. 579-589, Pergamon Press

[13] Margolis, D.L., and Brown, F.T., "Measurement of the Propagation of Long-Wavelength Disturbances through Turbulent Flow in Tubes", J. of Fluid Engineering, Trans. of the ASME, March. 1976, p. 70-78

[14] Wood, D.J., and Funk, J.E., "A Boundary-Layer Theory for Transient Viscous losses in Turbulent Flow", Journal of Basic Engineering, ASME, 1970, pp. 865-873

[15] Ohmi, M., Kyomen, S., and Usui, T., "Analysis of Velocity Distribution in Pulsating Turbulent Pipe Flow with Time-Dependent Friction Velocity", Bulletin of the JSME, Vol. 21, No. 157, July, 1978

[16] Ohmi, M., Iguchi, M., Usui, T., and Minami, H., "Flow Pattern and Frictional Losses in Pulsating Pipe Flow: Part 1 Effect of Pulsating

Frequency on the Turbulent Flow Pattern", Bulletin of the JSME, Vol. 23, No. 186, Dec. 1980

[17] Ohmi, M., and Iguchi, M., "Flow Pattern and Frictional Losses in Pulsating Pipe Flow: Part 2 Effect of Pulsating Frequency on the Turbulent Frictional Losses", Bulletin of the JSME, Vol. 23, No. 186, Dec. 1980

[18] Ohmi, M., and Iguchi, M., "Flow Pattern and Frictional Losses in Pulsating Pipe Flow: Part 3 General Representation of Turbulent Flow Pattern", Bulletin of the JSME, Vol. 23, No. 186, Dec. 1980

[19] Ohmi, M., and Iguchi, M., "Flow Pattern and Frictional Losses in Pulsating Pipe Flow: Part 4 General Representation of Turbulent Frictional Losses", Bulletin of the JSME, Vol. 24, No. 187, Jan. 1981

[20] Ohmi, M., Iguchi, M., and Usui, T., "Flow Pattern and Frictional Losses in Pulsating Pipe Flow: Part 5 Wall Shear Stress and Flow Pattern in a Laminar Flow", Bulletin of the JSME, Vol. 24, No. 187, Jan. 1981

[21] Ohmi, M., and Iguchi, M., "Flow Pattern and Frictional Losses in Pulsating Pipe Flow: Part 6 Frictional Losses in a Laminar Flow", Bulletin of the JSME, Vol. 24, No. 196, Oct. 1981

[22] Ohmi, M., and Iguchi, M., "Flow Pattern and Frictional Losses in Pulsating Pipe Flow: Part 7 Wall Shear Stress in a Turbulent Flow", Bulletin of the JSME, Vol. 24, No. 196, Oct. 1981

[23] Ohmi, M., Kyomen, S., and Usui, T., "Numerical Analysis of Pressure and Velocity Distributions for a Pulsating Turbulent Flow in a Circular

Tube Containing a Slightly Compressible Fluid", Bulletin of the JSME, Vol. 24, No. 187, Jan. 1981

[24] Ohmi, M., Kyomen, S., and Usui, T., "Numerical Analysis of Transient Turbulent Flow in a Liquid Line", Bulletin of JSME, 1985, Vol. 28(239), pp. 799-806

[25] Ohmi, M., Kyomen, S., and Usui, T., "Numerical Analysis of Transient Turbulent Flow in a Liquid Line", Bulletin of the JSME, Vol. 28, No. 239, May. 1985

[26] Bratland, O., "Frequency-Dependent Friction and Radial Kinetic Energy Variation in Transient Pipe Flow", 5th Int. Conf. on Pressure Surges, Hannover, F.R. Germany: 22-24, Sep. 1986

[27] Eichinger, P., and Lein, G., "The Influence of Friction on Unsteady Pipe Flow", Unsteady Flow and Fluid Transients, Bettess & Watts (eds), 1992, Balkema, Rotterdam, ISBN 90 5410 046 X

[28] Vardy, A.E., and Hwang K.L., "A Characteristics Model of Transient Friction in Pipes", Journal of Hydraulic Research, IAHR, 1991, Vol. 29(5), pp. 669-684

[29] Zhou, R.Q.N., "Modeling of Acoustic Phenomena in Reacting Piping, Part 5: Prediction of Volumetric Drag for Turbulent Pipe Flow", AECL Report, 1995, ARD-TD-465, COG-93-402

[30] Silva-Araya, W.F., and Chaudhry, M.H., "Computation of Energy Dissipation in Transient Flow", J. of Hydraulic Engineering, p. 108-115, Feb. 1997

[31] Pezzinga, G., "Quasi-2D Model for Unsteady Flow in Pipe networks", J. of Hydraulic Engineering, July 1999, p. 676-685

[32] Zielke, W., "Frequency-Dependent Friction in Transient Pipe Flow", Journal of Basic Engineering, ASME, 1968, pp. 109-115

[33] Trikha, A.K., "An Efficient Method for Simulating Frequency-Dependent Friction in Transient Liquid Flow", ASME Trans., J. Fluids Eng., 91:(1) p. 97-105, March 1975

[34] Kagawa, T., Lee, I., Kitagawa, A., and Takenaka, T., "High Speed and Accurate Computing Method of Frequency-Dependent Friction in Laminar Pipe Flow for Characteristics Method", TRANS. JSME, 1983, Vol. 49, No. 447, p2638

[35] Brown, F.T., "On Weighting Functions for the Simulation of Unsteady Turbulent Flow", Forum on Unsteady Flow, ASME, New Orleans, USA, 1984, FED-Vo. 15, pp.26-28

[36] Suzuki, K., Taketomi, T., and Sato, S., "Improving Zielke's Method of Simulating Frequency-Dependent Friction in Laminar Liquid Pipe Flow", Journal of Fluids Engineering, ASME, 1991, Vol. 113(4), pp. 569-573

[37] Vardy, A.E., "Approximating Unsteady Friction at High Reynolds numbers", Proc., Int. Conf. on Unsteady Flow and Fluid Transients, Durham, England, 1992, pp. 21-29

[38] Vardy, A.E., Hwang, K.L., and Brown, J.M.B., "A Weighting Function Model of Transient Turbulent Pipe Flow", Journal of Hydraulic Research, IAHR, 1993, pp. 533-548

[39] Schohl, G.A., "Improved Approximate Method for Simulating Frequency-Dependent Friction in Transient Laminar Flow", J. of Fluid Engineering, Trans. of the ASME, Sept. 1993, Vol. 115, p. 420-424

[40] Shuy, E.B., "Approximate Wall Shear Stress Equation for Unsteady Laminar Pipe Flows", J. of Hydraulic Research, Vol. 33, 1995, No. 4

[41] Vardy, A.E., and Brown, J.M.B., "Transient, Turbulent, Smooth pipe flow", Journal of Hydraulic Research, IAHR, 1995, pp. 435-456

[42] Vardy, A.E., and Brown, J.M.B., "On Turbulent, Unsteady, Smooth-Pipe Flow", Proc., Int. Conf. on Pressure Surges and Fluid Transients, BHR Group, Harrogate, England, 1996, pp. 289-311

[43] Brunone, B., Golia, U. M., and Greco, M., "Modeling of Fast Transients by Numerical Methods", Proc. 9th Round Table IAHR Group, Valentia, 1991, pp. 273-280

[44] Bughazem, M.B., and Anderson, A., "Problems with Simple Models for Damping in Unsteady Flow", Proc., Int. Conf. on Pressure Surges and Fluid Transients, BHR Group, Harrogate, England, 1996, pp. 537-548

[45] Brunone, B., Karney, B.W., Mecarelli, M., and Ferrante, M., "Velocity Profile And Unsteady Pipe Friction in Transient Flow", Journal of Water Resources Planning And Management, July/August 2000, pp. 236-244

[46] Vennatrø, B., "Unsteady Friction in Pipelines", Proc., XVIII IAHR Symposium on Hydraulic Machinery and Cavitation, Valencia, Spain, 1996, Vol. 2, pp. 819-826

[47] Svingen, B., "Rayleigh Damping as An Approximate Model for Transient Hydraulic Pipe Friction", Proc., 8th Int. Meet. on the Behaviour of Hydraulic Machinery under Steady Oscillatory Conditions, IAHR, Chatou, France, 1997, Paper F-2

[48] Young, T., "Propagation of Impulse Through an Elastic Tube", Tran. Royal Society of London, Vol. 98, 1808, pp. 164-186

[49] Wylie, E.B., "Frictional Effects in Unsteady Turbulent Pipe Flows", Appl. Mech. Rev., ASME, Vol 50, No. 11, part 2, Nov. 1997

[50] Chen, C., and Veshagh, A., "A Wall Friction Model for One-Dimensional Unsteady Turbulent Pipe Flows", Int. Congress and Exposition, SAE, Detroit, Michigan, March 1-5, 1993

[51] Suo, L., and Wylie, E.B., "Impulse Response Method for Frequency-Dependent Pipeline Transients", J. of Fluids Engineering, Trans. Of the ASME, Vol. 111, Dec. 1989, p. 478-483

[52] Goodson, R.E., and Leonard, R.G., "A Survey of Modeling Techniques for Fluid Line Transients", Journal of Basic Engineering, ASME, June/1972, pp. 474-482

[53] Bergant, A., Simpson, A.R., and Vítkovský, J., "Developments in Unsteady Pipe Flow Friction Modelling", Journal of Hydraulic Research, Vol. 39, 2001, No. 3, pp. 249-257

[54] Bergant, A., and Tijsseling, A., "Parameters Affecting Water Hammer Wave Attenuation, Shape and Timing", 10th International Meeting of the Work Group on THE BEHAVIOR OF HYDRAULIC MACHINERY

UBDER STEADY OSCILLATORY CONDITION, June 2001, Trondheim, Norway

[55] Chatoorgoon, V., Hau, K., Lee, N., and Reesor, G., "Modelling of Acoustic Phenomena in Reactor Piping, Part 1: Fundamental Studies", AECL Report, Dec. 1993, ARD-TD-465, COG-93-402

[56] Zhou, R.Q.N., and Chatoorgoon, V., "Modelling of Acoustic Phenomena in Reactor Piping, Part 2: Prediction of Acoustic Resonance in Tubes", AECL Report, July. 1997, ARD-TD-515, COG-94-471

[57] Chatoorgoon, V., and Zhou, R.., "Modelling of Acoustic Phenomena in Reactor Piping, Part 3: Fundamental Studies", AECL Report, Jan. 1995, ARD-TD-511, COG-94-464

[58] Sauer, R. E., "Transient Viscous Losses During Turbulent Flow of a Liquid in a Pipe", MS thesis, Department of Mechanical Engineering, University of Kentucky, Feb. 1969

[59] Iguchi, M., Ohmi, M., and Tanaka, S., "Experimental Study of Turbulence in a Pulsatile Pipe Flow", Bulletin of JSME, Vol. 28, No. 246, Dec. 1985

[60] Tu, S. W., and Ramaprian, B. R., "Fully Developed Periodic Turbulent Pipe Flow. Part 1. Main Experimental Results and Comparison with Prediction", J. of Fluid Mech., 1983, Vol. 137, pp. 31-58

[61] Hino, M., Sawamoto, M., and Takasu, S., "Experiments on Transition to Turbulent in an Oscillatory Pipe Flow", J. of Fluid Mech., 1976, Vol. 75, part 2, pp. 193-207

[62] Mizushina, T., Maruyama, T., and Shiozaki, Y., "Pulsating Turbulent Flow in a Tube", J. Chem. Engng Japan, June 1973, pp. 487-494

[63] Mizushina, T., Maruyama, T., and Hirasawa, H., "Structure of the Turbulence in Pulsating Pipe Flows", J. Chem. Engng Japan, Aug. 1975, pp. 210-216

[64] Kirmse, R. E., "Investigations of Pulsating Turbulent Pipe Flow", ASME Paper 79-WA/FE-1, 1979

[65] Kita, Y., Adachi, Y., and Hirose, K., "Periodically Oscillating Turbulent Flow in a Pipe", Bull. JSME 23, 1980, pp. 656-664

[66] Ohmi, M., Usui, T., Tanaka, O., and Toyama, M., "Pressure and Velocity distribution in Pulsating Turbulent Pipe Flow", Bull. JSME 19, 1976, pp.951-957

[67] Ramaprian, B. R., and Tu, S. W., "An Experimental Study of Oscillatory Pipe Flow at Transitional Reynolds Numbers", J. Fluid Mech., 100, 1980, pp. 513-544

[68] Richardson , E.G., and Tyler, E., "The Transverse Velocity Gradient Near the Mouth of Pipes in Which Alternating or Continuous Flow of Air is Established", Proc. of the Physical Society of London, 42, 1929

[69] Holmboe, E. L., and Rouleau, W. T., "The Effect of Viscous Shear on Transients in Liquid Lines", J. of Basic Engineering, TRANS. ASME, Series D, Vol. 89, No. 1, March 1967, pp. 174-180

[70] Budny, D. D., Wiggert, D. C., and Hatfield, F. J., "The Influence of Structural Damping on Internal Pressure During a Transient Pipe Flow", J. of Fluids Engineering, TRANS. ASME, Vol. 113, Sep. 1991, pp. 424-429

[71] Bergant, A., Simpson, A.R., and Vítkovský, J., "Review of Unsteady Friction Models in Transient Pipe Flow", Proceedings of the 9th International Meeting of the IAHR Work Group on the Behaviour of Hydraulic Machinery under Steady Oscillatory Conditions, Brno, Czech Republic, Paper D 1, 1999

[72] Elansary, A. S., Silva, W., and Chaudhry, M. H., "Numerical and Experimental Investigation of Transient Pipe Flow", J. of Hydraulic Research, Vol. 32, 1994, No. 5

[73] Simpson, A. R., and Bergant, A., "Column Separation Research at the University of Adelaide, South Australia", Int. Meeting on Hydraulic Transients with Column Separation, 9th Round Table, IAHR, Valencia, Spain, 352-366

[74] Modica, C., and Pezzinga, G., "Un Modello Quasi Bidimensionale per il Moto Vario Elastico in Regime Turbulento", Atti, XXIII Convegno di Idraulica e Costruzioni Idrauliche, Florence, Italy, E191-E205 (in Italian), 1992

[75] Brunon, B., and Morelli, L., "Automatic Control Valve-Induced Transients in Operative Pipe System", J. of Hydraulic Engineering, May 1999, pp. 534-542

[76] Carstens, M. R., and Roller, J. E., "Boundary-Shear Stress in Unsteady Turbulent Pipe Flow", J. of Hydraulics Division, Proceedings of the American Society of Civil Engineers, Feb. 1959, pp. 67-81

[77] Brunone, B., and Morelli, L., "Automatic Control Valve-Induced Transients in Operative Pipe System", J. Hydr. Engrg., ASCE, 1999, 125(5), pp. 534-542

[78] Zielke, W., Wylie, E. B., and Keller, R. B., "Forced and Self-Excited Oscillations in Propellant Lines", J. of Basic Engineering, TRANS. ASME, Dec. 1969, pp. 671-677

[79] Morgentroh, M., and Weaver, D. S., "Sound Generation by a Centrifugal Pump at Blade Passing Frequency", J. of Turbomachinery, TRANS. ASME, Vol. 120, Oct. 1998, pp. 736-743

[80] Morgentroh, M., and Weaver, D. S., "Acoustic Pressure Pulsations of a Centrifugal Volute Pump in a Pipeline", 3rd International Conference, Czech Committee of the European Mechanics Society Conference, Engineering Aero-Hydroelasticity, Prague, Aug. 30- Sep. 3, 1993, pp. 111-116

[81] Rzentkowski, G., and Zbroja, S., "Experimental Characterization of Centrifugal Pumps as an Acoustic Source at the Blade-Passing Frequency", J. of Fluids and Structures, 2000, Vol. 14, pp. 529-558

[82] Stirnemann, A., Eberl, J., Bolleter, U., and Pace, S., "Experimental Determination of the Dynamic Transfer Matrix for a Pump", J. of Fluids Engineering, TRANS. ASME, Vol. 109, Sep. 1987, pp. 218-225

[83] Washio, S., and Konishi, T., "Research on Wave Phenomena in Hydraulic Lines", Bulletin of JSME, Vol. 28, No. 241, July 1985

[84] Rzentkowski, G., Forest, J.W., and Russell, J.H., "Estimation of Pump-Generated Pressure Pulsations From Instrument Line Measurements", 1st International Symposium of PUMP NOISE AND VIBRATIONS, July 1993, Topic 8, pp. 397-409

[85] Kar, P.K., "Reactor Fuel Damage Computer Modelling and Analysis Work Program Review", Report of Nuclear Support Services Department, Feb. 1993, No. 938011

[86] Hadaller, G. I., Sawala, R. M., and Sandig, P. F., "Darlington N12 Acoustic Model Validation Tests in the Stern Loop With and Without Thirty-seven Element Fuel", Stern Sept., SL-064, March 1994

[87] Wylie, E.B., and Streeter, V.L., "Fluid Transients", New York : McGraw-Hill International Book Co., c1978

[88] Julius S. Bendat and Allan G. Piersol, "Random Data Analysis And Measurement Procedures", 2nd Edition, John Wiley & Sons.

APPENDIX A:

Experimental Data of The '7.03 m Dead-End Experiment'

Fluid	Water	Static Pressure (MPa)	0.4
Averaged Temperature (°C)	4.02	Measured Sound Speed (m/s)	1362.31

Time	Temperature (°C)	Frequency Range (Hz)
1/23/2005 18:00	3.90	2-174
1/23/2005 19:00	3.90	
1/23/2005 21:00	3.90	
1/28/2005 16:00	3.90	
1/28/2005 18:00	3.90	
1/28/2005 22:00	3.90	
1/28/2005 23:00	3.90	
1/30/2005 18:30	3.90	
1/30/2005 19:30	4.44	176-242
1/30/2005 20:30	4.44	
1/30/2005 21:30	4.44	
1/30/2005 22:30	4.44	
3/25/2005 19:40	4.44	
3/25/2005 20:30	3.90	244-500
3/25/2005 21:30	3.90	
3/25/2005 22:00	3.90	
3/25/2005 22:20	3.90	

Frequency (Hz)	P_1/P_0	Frequency (Hz)	P_1/P_0
2.00	9.9888E-01	34.00	2.7522E+00
4.00	1.0049E+00	36.00	3.3589E+00
6.00	1.0154E+00	38.00	4.3960E+00
8.00	1.0322E+00	40.00	6.2655E+00
10.00	1.0563E+00	42.00	1.0956E+01
12.00	1.0868E+00	44.00	1.6544E+01
14.00	1.1252E+00	44.25	1.9652E+01
16.00	1.1721E+00	44.50	2.2698E+01
18.00	1.2295E+00	44.75	2.2978E+01
20.00	1.3021E+00	45.00	2.3049E+01
22.00	1.3922E+00	45.25	2.3763E+01
24.00	1.5001E+00	45.50	2.4146E+01
26.00	1.6369E+00	45.75	2.4934E+01
28.00	1.8079E+00	46.00	2.5752E+01
30.00	2.0340E+00	46.25	2.6679E+01
32.00	2.3279E+00	46.50	2.6751E+01

Frequency (Hz)	P_1/P_0	Frequency (Hz)	P_1/P_0
46.75	2.6615E+01	126.00	1.6775E+00
47.00	2.5992E+01	128.00	1.9678E+00
47.25	2.4493E+01	130.00	1.9857E+00
47.50	2.2391E+01	132.00	2.2303E+00
47.75	2.0116E+01	134.00	2.4984E+00
48.00	1.8577E+01	136.00	2.8772E+00
50.00	8.7853E+00	138.00	3.4993E+00
52.00	5.5956E+00	140.00	4.2734E+00
54.00	4.0361E+00	142.00	5.6424E+00
56.00	3.2232E+00	144.00	8.0635E+00
58.00	2.6591E+00	146.00	1.2612E+01
60.00	2.2597E+00	147.00	1.5491E+01
62.00	1.9951E+00	147.25	1.7412E+01
64.00	1.8044E+00	147.50	2.2436E+01
66.00	1.6390E+00	147.75	1.7946E+01
68.00	1.4720E+00	148.00	1.7749E+01
70.00	1.3477E+00	148.25	1.7588E+01
72.00	1.2753E+00	148.75	1.5155E+01
74.00	1.2649E+00	150.00	1.2591E+01
76.00	1.1500E+00	152.00	1.0560E+01
78.00	1.0900E+00	154.00	8.5000E+00
80.00	1.0897E+00	156.00	7.3969E+00
82.00	9.9802E-01	158.00	5.8658E+00
84.00	9.5702E-01	160.00	4.7494E+00
86.00	9.2601E-01	162.00	3.9498E+00
88.00	8.9577E-01	164.00	3.3918E+00
90.00	8.9100E-01	166.00	2.8897E+00
92.00	8.7965E-01	168.00	2.4693E+00
94.00	8.6927E-01	170.00	2.1508E+00
96.00	8.7035E-01	172.00	1.9092E+00
98.00	8.6077E-01	174.00	1.7013E+00
100.00	8.6000E-01	176.00	1.5391E+00
102.00	8.7000E-01	178.00	1.4190E+00
104.00	8.8000E-01	180.00	1.2814E+00
106.00	8.9407E-01	182.00	1.1393E+00
108.00	9.5031E-01	184.00	1.0497E+00
110.00	9.8625E-01	186.00	9.7258E-01
112.00	1.0366E+00	188.00	8.8632E-01
114.00	1.0472E+00	190.00	8.5686E-01
116.00	1.1584E+00	192.00	8.1974E-01
118.00	1.2506E+00	194.00	8.1884E-01
120.00	1.3713E+00	196.00	8.1724E-01
122.00	1.4413E+00	198.00	8.1708E-01
124.00	1.5500E+00	200.00	8.2286E-01

Frequency (Hz)	P_1/P_0	Frequency (Hz)	P_1/P_0
202.00	8.3001E-01	264.00	3.1505E+00
204.00	8.4969E-01	266.00	2.5600E+00
206.00	8.6978E-01	268.00	2.0432E+00
208.00	9.1012E-01	270.00	1.8104E+00
210.00	9.5671E-01	272.00	1.5253E+00
212.00	1.0169E+00	274.00	1.4219E+00
214.00	1.0990E+00	276.00	1.2594E+00
216.00	1.1868E+00	278.00	1.1132E+00
218.00	1.2596E+00	280.00	1.0515E+00
220.00	1.3535E+00	282.00	9.4860E-01
222.00	1.4899E+00	284.00	9.0121E-01
224.00	1.6498E+00	286.00	8.3679E-01
226.00	1.7749E+00	288.00	7.9001E-01
228.00	2.0002E+00	290.00	7.7000E-01
230.00	2.1635E+00	292.00	7.6500E-01
232.00	2.3901E+00	294.00	7.5600E-01
234.00	2.6497E+00	296.00	7.5100E-01
236.00	3.0270E+00	298.00	7.4800E-01
238.00	3.4011E+00	300.00	7.4300E-01
240.00	3.9397E+00	302.00	7.4060E-01
242.00	4.5755E+00	304.00	7.3919E-01
244.00	5.4648E+00	306.00	7.4192E-01
246.00	7.0208E+00	308.00	7.5287E-01
247.25	8.9205E+00	310.00	7.7422E-01
247.50	9.1526E+00	312.00	7.8922E-01
247.75	9.5540E+00	314.00	8.2979E-01
248.00	1.0877E+01	316.00	8.6993E-01
248.25	1.0594E+01	318.00	9.2197E-01
248.50	1.0997E+01	320.00	9.7964E-01
248.75	1.1743E+01	322.00	1.0700E+00
249.00	1.2354E+01	324.00	1.1283E+00
249.25	1.3138E+01	326.00	1.2599E+00
249.50	1.3738E+01	328.00	1.3500E+00
249.75	1.5155E+01	330.00	1.4645E+00
250.00	1.8509E+01	332.00	1.6298E+00
250.25	1.7691E+01	334.00	1.8108E+00
250.50	1.7301E+01	336.00	2.1026E+00
250.75	1.6673E+01	338.00	2.5937E+00
252.00	1.4785E+01	340.00	3.1030E+00
254.00	1.3455E+01	342.00	3.8820E+00
256.00	1.1453E+01	344.00	4.6180E+00
258.00	7.8166E+00	346.00	5.8370E+00
260.00	5.4296E+00	348.00	7.0351E+00
262.00	3.9601E+00	350.00	8.3470E+00

Frequency (Hz)	P_1/P_0	Frequency (Hz)	P_1/P_0
350.25	8.7389E+00	412.00	6.9102E-01
350.50	8.9948E+00	414.00	7.1105E-01
350.75	9.3941E+00	416.00	7.2603E-01
351.00	1.0619E+01	418.00	7.5299E-01
351.25	1.1085E+01	420.00	7.7397E-01
351.50	1.1734E+01	422.00	8.0095E-01
351.75	1.2278E+01	424.00	8.5203E-01
352.00	1.2897E+01	426.00	8.8404E-01
352.25	1.2583E+01	428.00	9.2900E-01
352.50	1.1888E+01	430.00	9.9301E-01
352.75	1.1120E+01	432.00	1.0340E+00
353.00	1.0573E+01	434.00	1.0730E+00
353.25	9.0380E+00	436.00	1.0530E+00
353.50	8.6381E+00	438.00	1.2440E+00
353.75	8.0329E+00	440.00	1.3890E+00
354.00	7.3790E+00	442.00	1.4930E+00
356.00	5.9429E+00	444.00	1.8048E+00
358.00	4.2039E+00	446.00	2.2371E+00
360.00	3.2991E+00	448.00	2.6481E+00
362.00	2.7382E+00	450.00	3.5732E+00
364.00	2.3211E+00	451.00	5.4428E+00
366.00	1.9880E+00	451.25	6.9586E+00
368.00	1.7939E+00	451.50	7.9059E+00
370.00	1.6529E+00	451.75	8.6869E+00
372.00	1.4569E+00	452.00	9.0762E+00
374.00	1.3430E+00	452.25	9.5711E+00
376.00	1.2030E+00	452.50	9.7895E+00
378.00	1.1380E+00	452.75	1.0385E+01
380.00	1.0460E+00	453.00	9.9437E+00
382.00	1.0009E+00	453.25	9.2207E+00
384.00	9.4996E-01	453.50	8.8552E+00
386.00	9.1300E-01	453.75	8.6188E+00
388.00	8.6203E-01	454.00	8.0868E+00
390.00	8.3195E-01	454.25	7.0109E+00
392.00	7.8194E-01	454.50	6.6841E+00
394.00	7.7595E-01	454.75	6.2909E+00
396.00	7.4296E-01	455.00	5.8669E+00
398.00	7.2099E-01	456.00	5.4729E+00
400.00	7.1099E-01	458.00	4.3821E+00
402.00	7.0293E-01	460.00	3.4071E+00
404.00	6.9097E-01	462.00	2.9968E+00
406.00	6.8301E-01	464.00	2.3371E+00
408.00	6.8098E-01	466.00	1.9309E+00
410.00	6.8200E-01	468.00	1.5690E+00

Frequency (Hz)	P_1/P_0	Frequency (Hz)	P_1/P_0
470.00	1.4071E+00	486.00	7.7131E-01
472.00	1.2352E+00	488.00	7.5816E-01
474.00	1.0991E+00	490.00	7.1034E-01
476.00	1.0421E+00	492.00	6.7113E-01
478.00	9.9494E-01	494.00	6.6793E-01
480.00	9.1319E-01	496.00	6.6571E-01
482.00	8.5079E-01	498.00	6.5378E-01
484.00	8.3102E-01	500.00	6.4895E-01

APPENDIX B:

Experimental Data of The '9.20 m Turbulent Experiment'

Fluid	Water	Static Pressure (MPa)	0.2
Averaged Temperature (°C)	4.66	Measured Sound Speed (m/s)	1364.69
Flow Rate (m/s)	2.42	Reynolds Number	11,514.94

Time	Temperature (°C)	Frequency Range (Hz)
2/16/2005 22:30	3.90	2-100
2/16/2005 23:00	3.90	
2/16/2005 23:30	3.90	
2/17/2005 0:00	3.90	
2/17/2005 0:30	4.44	102-200
2/17/2005 1:00	4.44	
2/17/2005 1:30	4.44	
2/17/2005 2:00	5.00	202-500
2/17/2005 2:30	5.00	
2/17/2005 3:00	5.00	
2/17/2005 3:30	5.00	
2/17/2005 4:00	5.00	
2/17/2005 4:30	5.00	
2/17/2005 5:00	5.00	
2/17/2005 5:30	5.00	
2/17/2005 6:00	5.00	
2/17/2005 7:00	5.00	
2/17/2005 7:30	5.00	

Frequency (Hz)	P_1/P_0	Frequency (Hz)	P_1/P_0
4.00	1.7613E-02	34.00	2.8460E-02
6.00	1.3998E-02	36.00	3.7135E-02
8.00	1.1987E-02	37.00	3.0733E-02
10.00	1.1700E-02	38.00	2.5856E-02
12.00	1.1528E-02	39.00	2.0710E-02
14.00	1.1271E-02	40.00	1.9632E-02
16.00	1.1300E-02	42.00	1.5852E-02
18.00	1.2356E-02	44.00	1.4600E-02
20.00	1.2800E-02	46.00	1.2400E-02
22.00	1.3568E-02	48.00	1.5200E-02
24.00	1.4863E-02	50.00	1.6685E-02
26.00	1.7088E-02	52.00	2.2592E-02
28.00	1.7749E-02	54.00	3.1466E-02
30.00	2.0470E-02	56.00	3.3064E-02
32.00	2.4954E-02	58.00	4.0851E-02

Frequency (Hz)	P_1/P_0	Frequency (Hz)	P_1/P_0
60.00	4.9920E-02	132.00	5.0062E-01
62.00	6.3234E-02	134.00	6.2979E-01
64.00	7.4593E-02	136.00	7.5893E-01
66.00	1.1352E-01	138.00	7.3495E-01
68.00	1.7066E-01	140.00	6.7163E-01
70.00	3.0686E-01	142.00	7.3363E-01
71.00	4.3692E-01	144.00	8.5422E-01
72.00	7.7501E-01	146.00	1.0795E+00
72.25	9.2860E-01	148.00	1.4480E+00
72.50	1.0433E+00	150.00	1.8183E+00
72.75	1.1066E+00	150.25	1.8111E+00
73.00	1.0488E+00	150.50	1.9796E+00
73.25	9.6407E-01	150.75	2.4871E+00
73.50	8.5776E-01	151.00	3.0918E+00
73.75	7.5609E-01	151.25	2.7173E+00
74.00	6.4303E-01	151.50	2.5361E+00
76.00	3.4676E-01	151.75	2.2238E+00
78.00	2.4775E-01	152.00	3.6140E+00
80.00	1.8358E-01	152.25	1.6637E+00
82.00	1.6656E-01	152.50	1.4891E+00
84.00	1.6472E-01	152.75	1.1758E+00
86.00	1.6030E-01	153.00	1.0493E+00
88.00	1.5959E-01	153.25	9.1139E-01
90.00	1.6380E-01	153.50	6.7876E-01
92.00	1.6889E-01	153.75	6.0667E-01
94.00	1.8131E-01	154.00	5.0582E-01
96.00	1.9871E-01	156.00	4.3141E-01
98.00	2.1844E-01	158.00	2.4172E-01
100.00	2.5140E-01	160.00	2.0733E-01
102.00	3.8001E-01	162.00	1.6720E-01
104.00	4.3179E-01	164.00	1.2860E-01
106.00	5.2718E-01	166.00	1.0798E-01
108.00	5.6037E-01	168.00	1.0208E-01
110.00	5.8125E-01	170.00	9.1645E-02
112.00	5.6503E-01	172.00	7.2113E-02
114.00	5.1936E-01	174.00	6.9965E-02
116.00	4.5030E-01	176.00	6.3637E-02
118.00	3.2891E-01	178.00	6.6767E-02
120.00	3.5997E-01	180.00	5.7815E-02
122.00	2.1625E-01	182.00	5.6177E-02
124.00	1.6001E-01	184.00	5.2352E-02
126.00	1.7536E-01	186.00	5.4245E-02
128.00	2.4329E-01	188.00	6.4002E-02
130.00	3.4293E-01	190.00	5.7545E-02

Frequency (Hz)	P_1/P_0	Frequency (Hz)	P_1/P_0
192.00	5.6721E-02	252.00	1.6690E-02
194.00	6.3571E-02	254.00	1.6028E-02
196.00	5.0057E-02	256.00	1.5207E-02
198.00	6.0123E-02	258.00	1.5301E-02
200.00	5.1798E-02	260.00	1.5700E-02
202.00	4.9883E-02	262.00	1.7804E-02
204.00	4.9844E-02	264.00	1.8062E-02
206.00	6.0416E-02	266.00	2.0682E-02
208.00	5.5571E-02	268.00	2.3271E-02
210.00	6.8572E-02	270.00	2.7447E-02
212.00	7.3100E-02	272.00	2.8870E-02
214.00	8.8301E-02	274.00	3.1146E-02
216.00	1.2590E-01	276.00	3.9224E-02
218.00	1.9966E-01	278.00	3.8281E-02
220.00	4.2431E-01	280.00	4.1880E-02
220.25	5.3421E-01	282.00	4.4120E-02
220.50	7.3397E-01	284.00	4.7920E-02
220.75	1.5613E+00	286.00	5.1525E-02
221.00	2.3216E+00	288.00	6.1266E-02
221.25	2.4755E+00	290.00	8.5380E-02
221.50	2.4569E+00	292.00	1.2115E-01
221.75	1.0701E+00	292.25	1.3710E-01
222.00	1.1156E+00	292.50	1.3631E-01
222.25	8.2699E-01	292.75	1.7395E-01
222.50	6.4477E-01	293.00	2.4913E-01
222.75	4.1245E-01	293.25	7.6413E-01
223.00	4.3162E-01	293.50	9.8724E-01
223.25	2.4668E-01	293.75	1.2457E+00
223.50	2.0843E-01	294.00	1.3017E+00
223.75	1.6965E-01	294.25	1.5732E+00
224.00	1.6467E-01	294.50	9.0661E-02
226.00	1.6152E-01	294.75	5.6655E-02
228.00	7.4764E-02	295.00	4.5880E-01
230.00	4.0205E-02	295.25	3.9875E-01
232.00	3.5410E-02	295.50	3.1329E-01
234.00	2.9107E-02	295.75	2.2248E-01
236.00	2.9002E-02	296.00	1.4187E-01
238.00	2.8897E-02	298.00	7.5302E-02
240.00	2.4717E-02	300.00	5.0756E-02
242.00	2.2501E-02	302.00	4.0092E-02
244.00	2.1128E-02	304.00	3.4088E-02
246.00	1.9700E-02	306.00	2.4349E-02
248.00	1.8700E-02	308.00	2.5841E-02
250.00	1.8608E-02	310.00	2.1072E-02

Frequency (Hz)	P_1/P_0	Frequency (Hz)	P_1/P_0
312.00	2.0160E-02	377.25	7.2311E-01
314.00	1.8201E-02	377.50	6.2370E-01
316.00	1.6017E-02	377.75	4.3289E-01
318.00	1.6581E-02	378.00	2.7410E-01
320.00	1.4182E-02	380.00	1.4390E-01
322.00	1.4032E-02	382.00	8.7706E-02
324.00	1.4116E-02	384.00	6.3903E-02
326.00	1.4295E-02	386.00	5.0712E-02
328.00	1.4531E-02	388.00	3.9719E-02
330.00	1.4701E-02	390.00	3.6400E-02
332.00	1.5095E-02	392.00	3.5849E-02
334.00	1.5594E-02	394.00	3.3201E-02
336.00	1.5920E-02	396.00	3.2240E-02
338.00	1.6691E-02	398.00	3.0686E-02
340.00	1.6701E-02	400.00	2.9153E-02
342.00	1.6679E-02	402.00	2.8893E-02
344.00	1.7752E-02	404.00	2.8403E-02
346.00	2.0216E-02	406.00	2.7800E-02
348.00	2.1415E-02	408.00	2.7201E-02
350.00	2.4954E-02	410.00	2.6043E-02
352.00	2.3470E-02	412.00	2.4119E-02
354.00	2.9539E-02	414.00	2.3601E-02
356.00	3.3295E-02	418.00	2.3326E-02
358.00	3.0767E-02	420.00	2.4791E-02
360.00	3.7802E-02	422.00	2.6655E-02
362.00	4.3196E-02	424.00	2.7982E-02
364.00	5.7698E-02	426.00	2.9965E-02
366.00	6.0997E-02	428.00	3.3487E-02
368.00	7.1501E-02	430.00	3.5105E-02
370.00	8.4590E-02	432.00	3.6508E-02
372.00	1.0691E-01	434.00	4.0024E-02
374.00	1.1990E-01	436.00	4.5885E-02
374.25	1.7881E-01	438.00	4.8471E-02
374.50	2.9742E-01	440.00	5.5697E-02
374.75	4.1931E-01	442.00	6.1385E-02
375.00	5.4370E-01	444.00	9.9223E-02
375.25	6.9440E-01	446.00	2.0623E-01
375.50	8.1969E-01	447.25	3.5409E-01
375.75	9.2430E-01	447.50	4.7536E-01
376.00	1.0927E+00	447.75	7.0758E-01
376.25	1.2033E+00	448.00	8.0716E-01
376.50	1.1231E+00	448.25	6.5882E-01
376.75	9.8190E-01	448.50	4.5631E-01
377.00	8.3240E-01	448.75	3.6338E-01

Frequency (Hz)	P_1/P_0	Frequency (Hz)	P_1/P_0
450.00	3.1619E-01	476.00	4.2264E-02
452.00	1.7485E-01	478.00	4.2109E-02
454.00	1.1083E-01	480.00	3.9732E-02
456.00	8.3794E-02	482.00	3.6810E-02
458.00	8.0728E-02	484.00	3.5923E-02
460.00	7.4716E-02	486.00	4.0202E-02
462.00	7.8753E-02	488.00	3.8079E-02
464.00	6.8334E-02	490.00	3.9618E-02
466.00	6.0392E-02	492.00	4.3129E-02
468.00	5.9800E-02	494.00	4.3598E-02
470.00	5.1613E-02	496.00	4.7025E-02
472.00	4.6707E-02	498.00	4.8552E-02
474.00	4.4364E-02	499.50	5.0154E-02

APPENDIX C:

Experimental Data of The '9.20 m 0-Flow Experiment'

Fluid	Water	Static Pressure (MPa)	0.2
Averaged Temperature (°C)	7.44	Measured Sound Speed (m/s)	1383.41
Flow Rate (m/s)	0	Reynolds Number	0

Time	Temperature (°C)	Frequency Range (Hz)
4/11/2005 17:30	7.22	2-250
4/11/2005 18:00	7.22	
4/11/2005 18:30	7.22	
4/11/2005 19:00	7.22	
4/11/2005 19:30	7.22	
4/11/2005 20:00	7.22	
4/11/2005 20:30	7.22	
4/11/2005 21:00	7.22	
4/12/2005 18:00	7.78	252-500
4/12/2005 18:30	7.78	
4/12/2005 19:00	7.78	
4/12/2005 19:30	7.78	
4/12/2005 20:00	7.78	

Frequency (Hz)	P_1/P_0	Frequency (Hz)	P_1/P_0
2.00	1.2846E-02	35.00	5.4100E-02
4.00	1.2800E-02	36.00	8.1400E-02
6.00	1.2873E-02	37.00	1.1510E-01
8.00	1.3100E-02	38.00	9.1500E-02
10.00	1.4500E-02	39.00	8.6500E-02
12.00	1.5100E-02	40.00	6.5370E-02
14.00	1.5273E-02	42.00	5.3270E-02
16.00	1.5009E-02	44.00	4.1840E-02
18.00	1.6700E-02	46.00	3.9939E-02
20.00	1.7742E-02	48.00	4.4263E-02
22.00	1.8319E-02	50.00	4.9483E-02
24.00	2.0803E-02	52.00	5.4779E-02
26.00	2.0917E-02	54.00	5.9734E-02
28.00	2.5371E-02	56.00	7.0279E-02
30.00	2.9489E-02	58.00	8.3180E-02
32.00	3.4837E-02	60.00	1.0255E-01
34.00	3.7600E-02	62.00	1.2757E-01

Frequency (Hz)	P_1/P_0	Frequency (Hz)	P_1/P_0
64.00	1.6830E-01	90.00	4.7413E-01
66.00	2.4909E-01	92.00	4.1057E-01
68.00	2.5463E-01	94.00	3.8411E-01
70.00	3.9186E-01	96.00	3.1029E-01
72.00	5.8396E-01	98.00	2.5147E-01
72.25	3.3513E-01	100.00	2.0387E-01
72.50	3.3578E-01	102.00	1.6847E-01
72.75	3.9548E-01	104.00	1.7761E-01
73.00	4.6563E-01	106.00	1.6679E-01
73.25	5.5062E-01	108.00	1.1370E-01
73.50	6.7946E-01	110.00	9.3111E-02
73.75	8.0629E-01	112.00	7.1614E-02
74.00	1.0297E+00	114.00	5.5207E-02
74.25	1.0779E+00	116.00	4.4186E-02
74.50	1.1384E+00	118.00	4.1370E-02
74.75	1.4683E+00	120.00	4.0180E-02
75.00	1.6708E+00	122.00	4.0551E-02
75.25	1.2265E+00	124.00	4.8812E-02
75.50	1.1135E+00	126.00	5.7148E-02
75.75	1.0779E+00	128.00	4.6559E-02
76.00	9.9184E-01	130.00	5.5976E-02
78.00	7.9163E-01	132.00	6.3387E-02
80.00	6.1581E-01	134.00	6.8710E-02
82.00	6.6498E-01	136.00	8.6766E-02
84.00	6.3760E-01	138.00	1.1692E-01
86.00	6.0590E-01	140.00	1.3265E-01
87.00	7.2009E-01	142.00	1.6087E-01
87.25	8.3162E-01	144.00	1.9687E-01
87.50	9.5432E-01	146.00	2.5619E-01
87.75	1.2038E+00	148.00	3.6127E-01
88.00	1.3458E+00	150.00	5.3168E-01
88.25	1.0149E+00	152.00	1.0724E+00
88.50	9.9698E-01	152.25	1.1378E+00
88.75	8.2457E-01	152.50	1.3194E+00
89.00	7.3837E-01	152.75	1.5952E+00
89.25	7.3472E-01	153.00	1.6212E+00
89.50	7.0512E-01	153.25	1.7212E+00
89.75	7.5418E-01	153.50	1.8621E+00

Frequency (Hz)	P_1/P_0	Frequency (Hz)	P_1/P_0
153.75	1.9300E+00	214.00	1.9569E-01
154.00	1.9293E+00	216.00	3.6559E-01
154.25	1.8922E+00	218.00	5.5463E-01
154.50	1.6762E+00	220.00	8.1470E-01
154.75	1.5193E+00	222.00	1.0740E+00
155.00	1.3590E+00	224.00	1.5311E+00
155.25	1.2293E+00	226.00	2.0622E+00
155.50	1.1257E+00	228.00	2.8688E+00
155.75	1.0086E+00	229.00	3.2185E+00
156.00	9.1414E-01	229.25	3.7134E+00
158.00	6.7764E-01	229.50	4.5358E+00
160.00	4.8306E-01	229.75	4.8834E+00
162.00	3.8905E-01	230.00	5.0113E+00
164.00	3.1405E-01	230.25	4.7090E+00
166.00	2.8062E-01	230.50	3.9395E+00
168.00	2.7766E-01	230.75	3.4092E+00
170.00	2.3573E-01	231.00	2.9340E+00
172.00	2.1845E-01	232.00	2.8987E+00
174.00	2.1670E-01	234.00	2.2213E+00
176.00	2.2242E-01	236.00	1.5438E+00
178.00	1.9476E-01	238.00	1.3421E+00
180.00	1.7383E-01	240.00	1.0257E+00
182.00	1.7537E-01	242.00	9.0559E-01
184.00	2.0219E-01	244.00	8.5428E-01
186.00	2.3821E-01	246.00	6.7773E-01
188.00	2.4908E-01	248.00	5.5274E-01
190.00	2.1945E-01	250.00	4.7534E-01
192.00	1.8443E-01	252.00	3.9537E-01
194.00	1.4363E-01	254.00	3.2885E-01
196.00	1.2274E-01	256.00	2.6485E-01
198.00	1.0520E-01	258.00	2.1038E-01
200.00	1.0520E-01	260.00	1.5453E-01
202.00	1.0690E-01	262.00	1.2853E-01
204.00	1.0864E-01	264.00	1.0520E-01
206.00	1.1912E-01	266.00	1.1015E-01
208.00	1.4093E-01	268.00	9.9927E-02
210.00	1.6943E-01	270.00	9.7292E-02
212.00	2.5282E-01	272.00	9.6919E-02

Frequency (Hz)	P_1/P_0	Frequency (Hz)	P_1/P_0
274.00	1.0017E-01	334.00	1.9588E-01
276.00	9.6239E-02	336.00	2.1186E-01
278.00	1.2295E-01	338.00	2.4625E-01
280.00	1.3308E-01	340.00	2.5150E-01
282.00	1.5241E-01	342.00	2.3265E-01
284.00	1.8578E-01	344.00	1.7231E-01
286.00	2.5063E-01	346.00	2.0471E-01
288.00	3.3993E-01	348.00	1.8866E-01
290.00	6.4269E-01	350.00	2.1958E-01
292.00	1.1194E+00	352.00	2.1536E-01
294.00	1.7579E+00	354.00	2.1122E-01
296.00	2.9377E+00	356.00	2.2182E-01
298.00	4.7534E+00	358.00	2.2198E-01
300.00	5.4325E+00	360.00	3.0890E-01
302.00	7.2604E+00	362.00	3.6384E-01
303.00	8.3831E+00	364.00	3.8133E-01
303.25	8.9383E+00	366.00	5.6364E-01
303.50	9.4195E+00	368.00	9.5940E-01
303.75	1.0138E+01	370.00	1.3583E+00
304.00	1.1038E+01	372.00	1.9031E+00
304.25	1.0517E+01	374.00	2.8379E+00
304.50	9.8476E+00	376.00	3.9446E+00
304.75	8.0517E+00	378.00	5.5302E+00
305.00	7.1508E+00	380.00	7.0338E+00
306.00	5.1055E+00	381.00	7.4393E+00
308.00	3.9394E+00	381.25	8.5808E+00
310.00	2.4816E+00	381.50	9.5768E+00
312.00	1.8625E+00	381.75	9.6277E+00
314.00	1.2417E+00	382.00	9.2172E+00
316.00	7.9068E-01	382.25	8.5483E+00
318.00	5.4570E-01	382.50	7.4437E+00
320.00	4.0179E-01	382.75	7.3944E+00
322.00	3.0761E-01	383.00	6.5584E+00
324.00	2.7773E-01	384.00	4.6455E+00
326.00	2.5586E-01	386.00	3.3416E+00
328.00	2.6566E-01	388.00	2.1777E+00
330.00	1.9187E-01	390.00	1.7172E+00
332.00	2.2594E-01	392.00	1.7216E+00

Frequency (Hz)	P_1/P_0	Frequency (Hz)	P_1/P_0
394.00	1.7204E+00	456.00	2.0277E+00
396.00	2.3192E+00	458.00	2.7606E+00
398.00	2.6467E+00	460.00	3.5083E+00
400.00	2.3123E+00	460.25	3.7581E+00
402.00	1.9486E+00	460.50	3.8218E+00
404.00	2.3082E+00	460.75	4.3287E+00
406.00	1.4454E+00	461.00	4.8477E+00
408.00	8.6670E-01	461.25	4.0169E+00
410.00	6.3513E-01	461.50	3.8100E+00
412.00	5.3054E-01	461.75	3.7534E+00
414.00	4.4978E-01	462.00	3.3674E+00
416.00	4.6147E-01	464.00	2.5942E+00
418.00	4.9128E-01	466.00	2.1135E+00
420.00	5.2921E-01	468.00	2.0426E+00
422.00	5.2093E-01	470.00	1.5850E+00
424.00	4.2868E-01	472.00	1.1683E+00
426.00	4.3215E-01	474.00	9.5060E-01
428.00	3.8730E-01	476.00	7.5054E-01
430.00	3.7432E-01	478.00	6.7548E-01
432.00	4.5631E-01	480.00	7.3292E-01
434.00	6.2078E-01	482.00	8.7101E-01
436.00	6.6559E-01	484.00	9.1928E-01
438.00	7.4871E-01	486.00	9.0612E-01
440.00	8.8427E-01	488.00	7.9408E-01
442.00	1.0649E+00	490.00	7.1497E-01
444.00	1.1223E+00	492.00	6.0228E-01
446.00	1.2371E+00	494.00	5.8809E-01
448.00	1.2324E+00	496.00	5.6996E-01
450.00	1.3139E+00	498.00	6.2330E-01
452.00	1.6322E+00	500.00	5.4439E-01
454.00	1.9520E+00		

APPENDIX D:

Calibration Certificates of Dynamic Pressure Transducers

Calibration Certificate of The Pressure Transducer P_0

CALIBRATION CERTIFICATE

Model:	112A22				
Serial #:	22869	Nat'l Freq:	300 kHz	Date:	1/9/04
Description:	Pressure Sensor			By:	Eric Kachermeyer, Cal. Tech
Type:	ICP	Time Constant:	2.8 sec	Station:	903 Pulse #1 (Test procedure AT601-6)
Sensitivity*:	98.67 mV/PSI			Temp:	71 deg F [22deg C]
	14.31 mV/kPa			Humidity:	9 %
Linearity*:	0.2% FS			Cert #:	160833
Uncertainty**:	+/- 0.64 %				

Bias: 8.4 VDC

* Zero based, least-squares straight line.

** Measurement uncertainty represented using a coverage factor of k=2 which provides a level of confidence of approximately 95 %.

Condition of Unit:
As Found: Not applicable
As Left: In tolerance, new unit

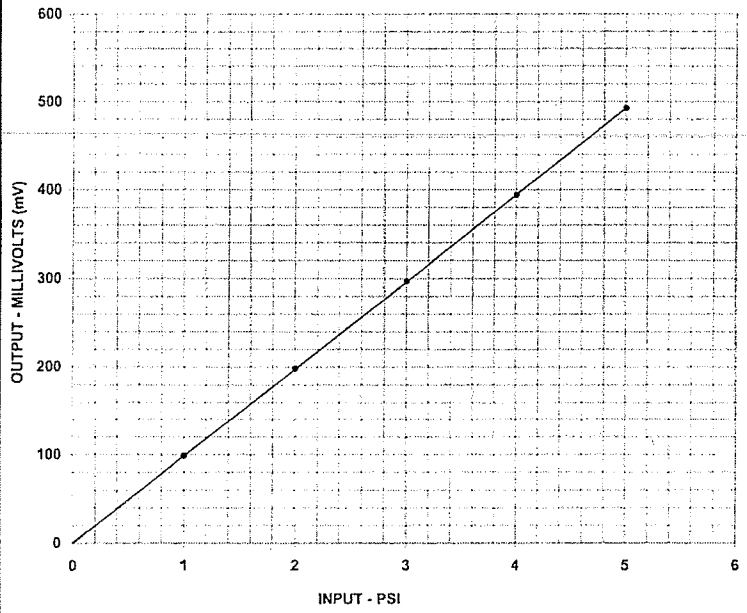

TEST DATA

INPUT (PSI)	OUTPUT (mV)
1.00	99
2.00	198
3.00	297
4.00	394
5.00	493

Notes:
1 STATION #15
2 Calibration is traceable to NIST and is accredited to ISO 17025 and ANSI/NCSL Z540-1-1994.
3 NIST traceability through PCB control # CA215.
4 This certificate may not be reproduced, except in full, without written approval from PCB Piezotronics, Inc.

ACCREDITED
Cert. No. 1862.01

PCB PIEZOTRONICS

Tel: 716-684-0001 Fax: 716-684-0987 Email: sales@pcb.com
3425 Walden Avenue, Depew NY 14043

ISO 9001 CERTIFIED

Page 1 of 1

Calibration Certificate of The Pressure Transducer P_0 (Cont'd)

CALIBRATION CERTIFICATE

Model:	112A22				
Serial #:	22869	**Nat'l Freq:**	300 kHz	**Date:**	1/9/04
Description:	Pressure Sensor			**By:**	Eric Kachenmeyer, Cal. Tech
Type:	ICP	**Time Constant:**	2.8 sec	**Station:**	903 Pulse #1 (Test procedure AT601-6)
Sensitivity*:	99.45 mV/PSI			**Temp:**	71 deg F (22deg C)
	14.42 mV/kPa			**Humidity:**	9 %
Linearity*:	0.1% FS			**Cert #:**	160816
Uncertainty:**	+/- 0.64 %				

Bias: 8.4 VDC

* Zero based, least-squares straight line.

** Measurement uncertainty represented using a coverage factor of k=2 which provides a level of confidence of approximately 95 %.

Condition of Unit:
As Found: Not applicable
As Left: In tolerance, new unit

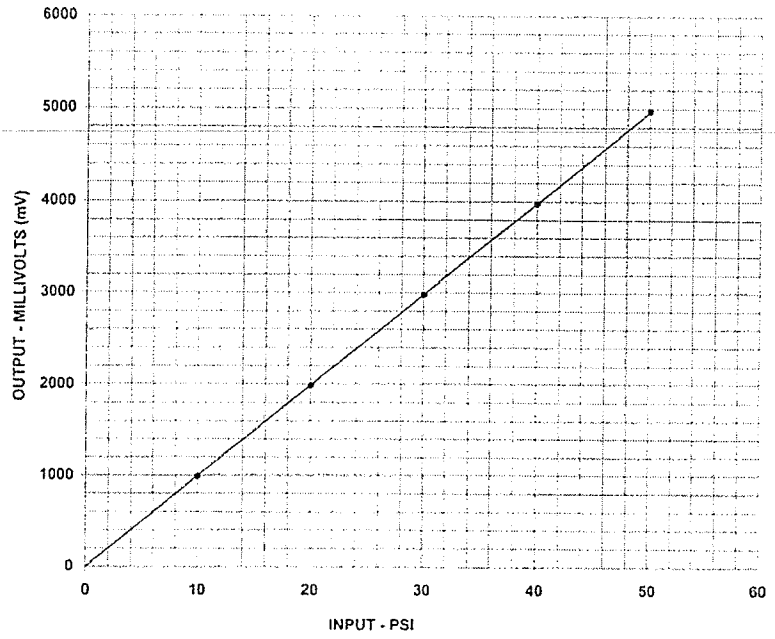

TEST DATA

INPUT (PSI)	OUTPUT (mV)
10.0	988
20.0	1985
30.0	2978
40.0	3979
50.0	4978

Notes:
1 STATION #15
2 Calibration is traceable to NIST and is accredited to ISO 17025 and ANSI/NCSL Z540-1-1994.
3 NIST traceability through PCB control # CA215.
4 This certificate may not be reproduced, except in full, without written approval from PCB Piezotronics, Inc.

ACCREDITED
Cert. No. 1862.01

PCB PIEZOTRONICS™

Tel: 716-684-0001 Fax: 716-684-0987 Email: sales@pcb.com
3425 Walden Avenue, Depew NY 14043

ISO 9001 CERTIFIED

Calibration Certificate of The Pressure Transducer P_1

CALIBRATION CERTIFICATE

Model:	112A22			Date:	1/9/04
Serial #:	22871	Nat'l Freq:	300 kHz	By:	Eric Kachermeyer, Cal. Tech
Description:	Pressure Sensor			Station:	903 Pulse #1 (Test procedure AT601-6)
Type:	ICP	Time Constant:	3 sec		
Sensitivity*:	98.84 mV/PSI 14.33 mV/kPa			Temp:	71 deg F [22deg C]
				Humidity:	9 %
Linearity*:	0.1% FS			Cert #:	160835
Uncertainty**:	+/- 0.64 %				

Bias: 8.2 VDC

* Zero based, least-squares straight line

** Measurement uncertainty represented using a coverage factor of k=2 which provides a level of confidence of approximately 95 %.

Condition of Unit:
As Found: Not applicable
As Left: In tolerance, new unit

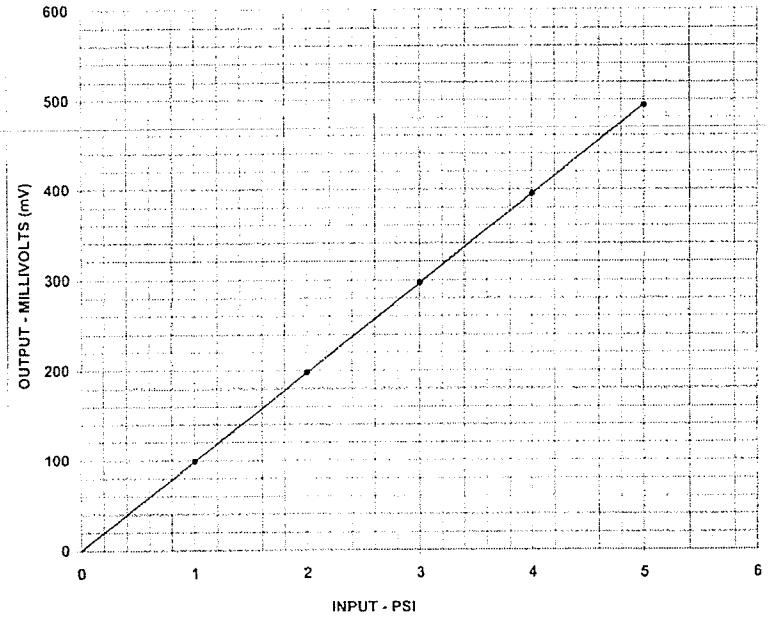

TEST DATA

INPUT (PSI)	OUTPUT (mV)
1.00	99
2.00	198
3.00	297
4.00	395
5.00	494

Notes:
1 STATION #15
2 Calibration is traceable to NIST and is accredited to ISO 17025 and ANSI/NCSL Z540-1-1994.
3 NIST traceability through PCB control # CA215.
4 This certificate may not be reproduced, except in full, without written approval from PCB Piezotronics, Inc.

ACCREDITED
Cert. No. 1862.01

PCB PIEZOTRONICS inc.
Tel: 716-684-0001 Fax: 716-684-0987 Email: sales@pcb.com
3425 Walden Avenue, Depew NY 14043

ISO 9001 CERTIFIED

Calibration Certificate of The Pressure Transducer P_1 (Cont'd)

CALIBRATION CERTIFICATE

Model:	112A22				
Serial #:	22871	Nat'l Freq:	300 kHz	Date:	1/9/04
Description:	Pressure Sensor			By:	Eric Kachermeyer, Cal. Tech
Type:	ICP	Time Constant:	3 sec	Station:	903 Pulse #1 (Test procedure AT601-6)
Sensitivity*:	99.89 mV/PSI 14.49 mV/kPa			Temp: Humidity:	71 deg F [22deg C] 9 %
Linearity*:	0.1% FS			Cert #:	160820
Uncertainty**:	+/- 0.64 %				

Bias: 8.2 VDC

* Zero based, least-squares straight line.

** Measurement uncertainty represented using a coverage factor of k=2 which provides a level of confidence of approximately 95 %.

Condition of Unit:
As Found: Not applicable
As Left: In tolerance, new unit

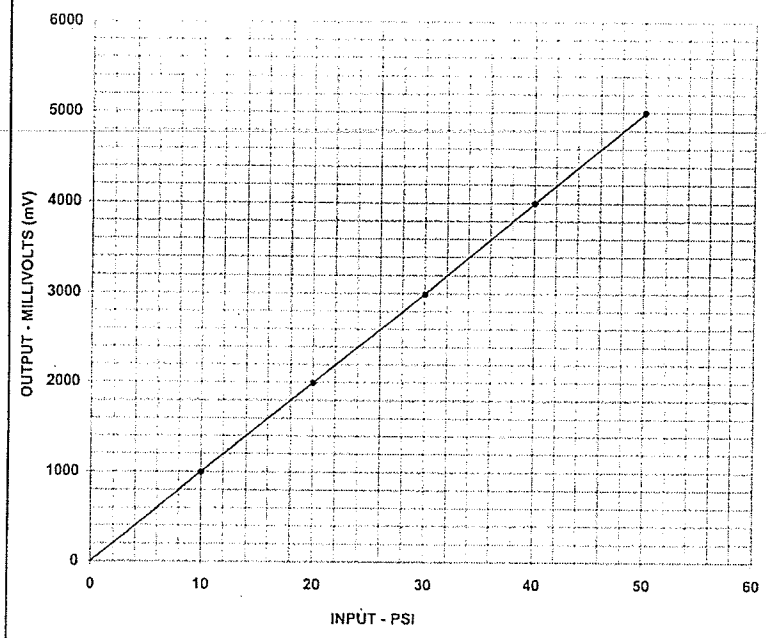

TEST DATA

INPUT (PSI)	OUTPUT (mV)
10.0	993
20.0	1994
30.0	2990
40.0	3997
50.0	5000

Notes:
1 STATION #15
2 Calibration is traceable to NIST and is accredited to ISO 17025 and ANSI/NCSL Z540-1-1994.
3 NIST traceability through PCB control # CA215.
4 This certificate may not be reproduced, except in full, without written approval from PCB Piezotronics, Inc.

ACCREDITED
Cert. No. 1862.01

PCB PIEZOTRONICS

Tel: 716-684-0001 Fax: 716-684-0987 Email: sales@pcb.com
3425 Walden Avenue, Depew NY 14043

ISO 9001 CERTIFIED

Page 1 of 1